Preparation of *ansa*-Niobocene and *ansa*-Tantalocene Olefin Hydride Complexes as Transition State Analogues in Metallocene-Catalyzed Olefin Polymerization

Paul J. Chirik,[1] Deanna L. Zubris,[2] Lily J. Ackerman, Lawrence M. Henling, Michael W. Day, and John E. Bercaw*

Arnold and Mabel Beckman Laboratories of Chemical Synthesis, California Institute of Technology, Pasadena, California 91125

Received August 2, 2002

To examine the effects of cyclopentadienyl and olefin substitution on preferred stereochemistry, a series of singly [$SiMe_2$]-bridged *ansa*-niobocene and -tantalocene olefin hydride complexes has been prepared via reduction and alkylation of the corresponding dichloride complexes. In this manner, [$Me_2Si(\eta^5\text{-}C_5H_4)(\eta^5\text{-}C_5H_3\text{-}3\text{-}R)$]$M(CH_2{=}CHR')H$ (M = Nb, Ta; R = $CHMe_2$, CMe_3; R′ = H, C_6H_5; M = Ta; R = $CHMe_2$, CMe_3; R′ = Me), *rac*- and *meso*-[$Me_2Si(\eta^5\text{-}C_5H_3\text{-}3\text{-}R)(\eta^5\text{-}C_5H_3\text{-}3\text{-}R)$]$Nb(CH_2{=}CH_2)H$ (R = CMe_3), and [$Me_2Si(\eta^5\text{-}C_5H_4)(\eta^5\text{-}C_5H_2\text{-}2,4\text{-}(CHMe_2)_2)$]$Ta(CH_2{=}CHR')H$ (R′ = H, C_6H_5) have been prepared and characterized by NMR spectroscopy and, in some cases, X-ray diffraction. The doubly [$SiMe_2$]-bridged *ansa*-tantalocene ethylene hydride complex [$(1,2\text{-}SiMe_2)_2(\eta^5\text{-}C_5H\text{-}3,5\text{-}(CHMe_2)_2)(\eta^5\text{-}C_5H_2\text{-}4\text{-}CMe_3)$]-$Ta(CH_2{=}CH_2)H$ has been prepared from thermolysis of the methylidene methyl complex [$(1,2\text{-}SiMe_2)_2(\eta^5\text{-}C_5H\text{-}3,5\text{-}(CHMe_2)_2)(\eta^5\text{-}C_5H_2\text{-}4\text{-}CMe_3)$]$Ta(CH_2)CH_3$. Addition of an excess of propylene or styrene to the tantalocene ethylene hydride results in olefin exchange and formation of the olefin hydride complexes [$(1,2\text{-}SiMe_2)_2(\eta^5\text{-}C_5H\text{-}3,5\text{-}(CHMe_2)_2)(\eta^5\text{-}C_5H_2\text{-}4\text{-}CMe_3)$]$Ta(CH_2{=}CHR')H$ (R′ = CH_3, C_6H_5). These compounds serve as stable transition state analogues for the much more kinetically labile group 4 metallocenium cationic intermediates in metallocene-catalyzed olefin polymerization. Characterization of the thermodynamically preferred isomers of metallocene olefin hydride complexes reveals that alkyl substitution on the cyclopentadienyl ligand array may have a significant effect on the stereochemistry of olefin coordination.

Introduction

Stereospecific olefin polymerization promoted by group 3 and 4 *ansa*-metallocene catalysts represents one of the most enantioselective chemical transformations known.[3] Elucidation of the steric and electronic factors that control this remarkable selectivity may aid in the design of new catalysts and also result in the development of new asymmetric transformations. Considerable effort has been devoted toward understanding the nature of the transition state for the C−C bond forming step with metallocene polymerization catalysts. The electronic requirements for an active catalyst are fairly well accepted: a metallocene alkyl with two vacant orbitals (Chart 1), where one orbital is used to accommodate the incoming olefin while the other allows for α-agostic assistance[4] in the transition state for carbon−carbon bond formation.[5]

Chart 1

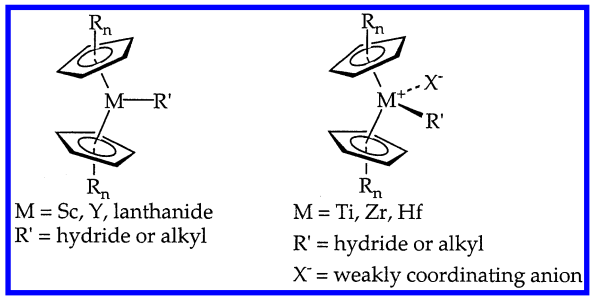

Understanding the key steric interactions in the olefin insertion transition state has also been the focus of many experimental and theoretical investigations. Calculations by Corradini[6] demonstrate that the enantiofacial approach of the olefin is determined by the orientation of the metal alkyl unit, such that the olefin substituent is placed in a trans relationship with the β-carbon of the metal polymeryl unit. The polymeryl is believed to orient toward the most open portion of the metallocene framework (Scheme 1; schematic view of C_2-symmetric metallocene looking into the wedge). The first experimental evidence in support of this model was

(1) Current address: Department of Chemistry and Chemical Biology, Cornell University, Ithaca, NY 14853-1301.

(2) Current address: Department of Chemistry, Villanova University, Villanova, PA 19085.

(3) For recent reviews see: (a) Brintzinger, H. H.; Fischer, D.; Mülhaupt, R.; Reiger, B.; Waymouth, R. M. *Angew. Chem., Int. Ed. Engl.* **1995**, *34*, 1143. (b) Bochmann, M. *J. Chem. Soc., Dalton Trans.* **1996**, 255.

(4) (a) Piers, W. E.; Bercaw, J. E. *J. Am. Chem. Soc.* **1990**, *112*, 9406. (b) Krauledat, H.; Brintzinger, H. H. *Angew. Chem., Int. Ed. Engl.* **1990**, *29*, 1412. (c) Grubbs, R. H.; Coates, G. W. *Acc. Chem. Res.* **1996**, *29*, 85.

(5) Jordan, R. F. *Adv. Organomet. Chem.* **1991**, *32*, 325.

(6) Guerra, G.; Cavallo, L.; Moscardi, G.; Vacetello, M.; Corradini, P. *J. Am. Chem. Soc.* **1994**, *116*, 2988.

10.1021/om020628d CCC: $25.00
Publication on Web 12/07/2002

Scheme 1

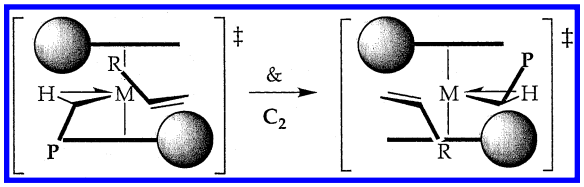

Scheme 2

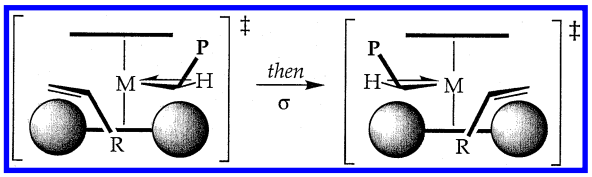

provided by Pino.[7] Hydrooligomerization of α-olefins with optically pure [ethylenebis(4,5,6,7-tetrahydroindenyl)]zirconium dichloride (EBTHIZrCl$_2$) produced chiral hydrotrimers and hydrotetramers with the predicted absolute configurations.[8] In contrast to polymerizations/oligomerizations, deuteriations of α-olefins such as styrene and pentene produced lower ee's with the opposite enantiofacial selectivity.[9] Similarly, work from our laboratories defined the diastereoselective transition structures for 1-pentene addition to yttrium−hydride and yttrium−pentyl bonds.[10] An optically pure, isotopically chiral 1-pentene was prepared and used to evaluate the stereoselectivity with an optically pure yttrocene. The absolute diastereoselectivities were established: insertion into the yttrium−hydride bond proceeds with modest selectivity (34% ee); insertion into the yttrium−pentyl bond proceeds via the other diastereomeric transition state with very high levels (>95% ee) of selectivity. Analogous transition state arguments have been proposed for the titanocene-catalyzed asymmetric hydrogenation of olefins reported by Buchwald and co-workers.[11]

The stereochemical model developed in the C_2-symmetric isospecific systems has since been extended to include C_s-symmetric syndiospecific catalysts.[12] The favored transition state geometry for syndiospecific catalysts is shown in Scheme 2 (schematic view of a C_s-symmetric metallocene looking into the wedge), where again the dominant stereo-directing interaction is a trans relationship between propylene methyl and the $C_\alpha-C_\beta$ bond of the polymer chain. Whether on the left or right side of the metallocene wedge, the growing polymer chain extends up and away from the more sterically demanding cyclopentadienyl moiety, thus forcing the propylene methyl group down. In syndiospecific catalysts, this lower cyclopentadienyl ligand contains an open region to accommodate the methyl substituent on the incoming monomer. Essential to the stereospecificity is a regular alternation of propylene

Scheme 3

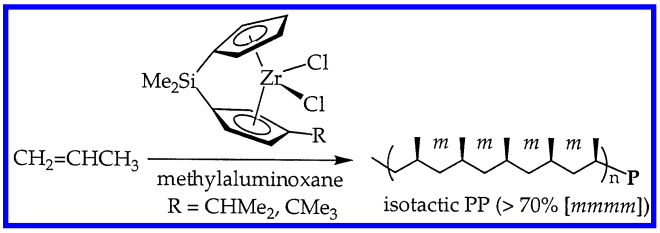

Scheme 4

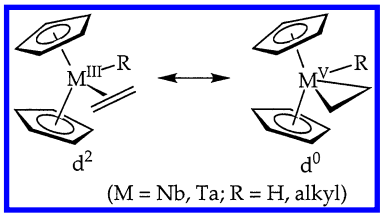

approach from one side of the metallocene wedge and then the other.[13]

Although these stereochemical models have been quite successful in explaining the high levels of stereocontrol observed with C_2- and C_s-symmetric catalysts, the stereospecificity of some metallocene catalysts cannot be readily rationalized. For example, the C_1-symmetric, monosubstituted, singly silylene-bridged zirconocene catalyst [Me$_2$Si(η^5-C$_5$H$_4$)(η^5-C$_5$H$_3$-3-R)]ZrCl$_2$/MAO (R = CMe$_3$, CHMe$_2$), originally reported by Miya,[14a] polymerizes propylene with [*mmmm*] contents exceeding 70% (Scheme 3). Obviously, the stereocontrol mechanisms of Schemes 1 and 2 do not apply, and thus one cannot readily explain such high isospecificity.

A possible approach to understanding the stereochemistry of olefin insertion would be to model the carbon−hydrogen or carbon−carbon bond-forming transition states of a group 4 metallocene catalyst using the *ground-state analog*, a (stable) group 5 (M = Nb, Ta) metallocene olefin hydride or olefin alkyl complex. These complexes have been used to investigate the steric and electronic effects for olefin insertion into metal−hydride bonds with bis(cyclopentadienyl) and related *ansa*-niobocene and -tantalocene olefin hydride complexes.[15] The niobocene and tantalocene complexes are formally M(III), d^2 metal centers (Scheme 4) that stabilize the olefin−metal bond through a strong π-back-bonding interaction.

Conventional NMR and X-ray diffraction experiments may be used to determine the structure of the metallocenes and thus to establish the direction and magnitude of steric effects (shown for one of the enantiomers of {[Me$_2$Si(η^5-C$_5$H$_4$)(η^5-C$_5$H$_3$-3-R^1)]M} in Chart 2). There are three stereoisomeric relationships between the olefin hydride complexes: (1) the preference for the olefin to be on the side of the metallocene wedge distal or proximal to the cyclopentadienyl substituent (R^1), (2) the preference for olefin coordination with its substituent (R^3) syn or anti to the substituted cyclopentadienyl

(7) Pino, P.; Cioni, P.; Wei, J. *J. Am. Chem. Soc.* **1987**, *109*, 6189.
(8) Pino, P.; Galimberti, M. *J. Organomet. Chem.* **1989**, *370*, 1.
(9) Waymouth, R.; Pino, P. *J. Am. Chem. Soc.* **1990**, *112*, 4911.
(10) Gilchrist, J. H.; Bercaw, J. E. *J. Am. Chem. Soc.* **1996**, *118*, 12021.
(11) (a) Broene, R. D.; Buchwald, S. L. *J. Am. Chem. Soc.* **1993**, *115*, 12569. (b) Troutman, M. V.; Appella, D. H.; Buchwald, S. L. *J. Am. Chem. Soc.* **1999**, *121*, 4916.
(12) Herzog, T. A.; Zubris, D. L.; Bercaw, J. E. *J. Am. Chem. Soc.* **1996**, *118*, 11988.
(13) Veghini, D.; Henling, L. M.; Burkhardt, T. J.; Bercaw, J. E. *J. Am. Chem. Soc.* **1999**, *121*, 564.
(14) (a) Mise, T.; Miya, S.; Yamazaki, H. *Chem. Lett.* **1989**, 1853. (b) Zhong, A. H.; Bercaw, J. E. Unpublished results.
(15) (a) Doherty, N. M.; Bercaw, J. E. *J. Am. Chem. Soc.* **1985**, *107*, 2670. (b) Burger, B. J.; Santarsiero, B. D.; Trimmer, M. S.; Bercaw, J. E. *J. Am. Chem. Soc.* **1988**, *110*, 3134. (c) Ackerman, L. J.; Green, M. L. H.; Green, J. C.; Bercaw, J. E. *Organometallics* **2003**, *22*, 188.

Chart 2

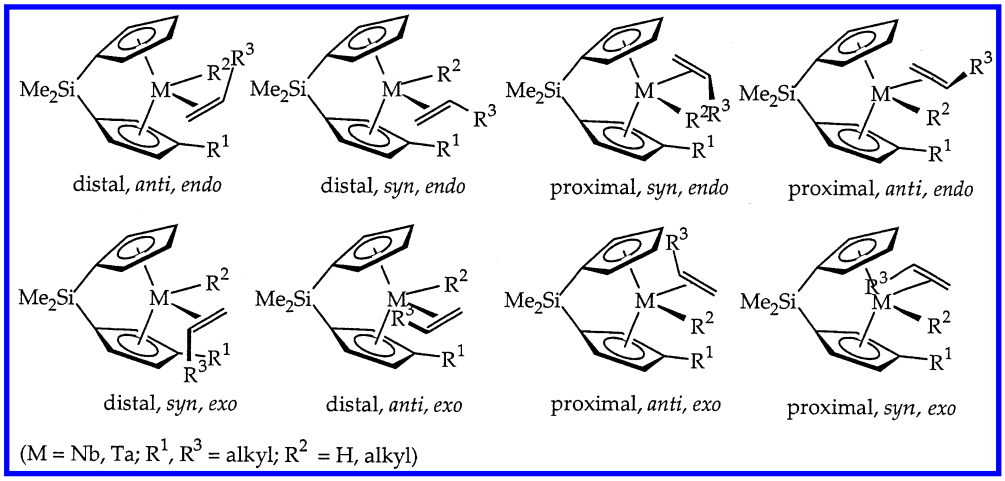

ring, and (3) the preference for the olefin substituent (R^3) to position itself endo or exo relative to the metallocene hydride or metallocene alkyl fragment (R^2).

Reports of group 5 *ansa*-metallocenes are limited and generally restricted to C_{2v}-symmetric metallocene frameworks,[16,17a,b,18–20] except for one report of C_1-symmetric *ansa*-niobocene imido complexes.[17c] In this report we describe the synthesis and characterization of a series of low-symmetry, singly and doubly [$SiMe_2$]-bridged group 5 metallocene olefin hydride complexes. The preferred structures of these complexes have been examined regarding the important stereodirecting interactions between the coordinated olefin and the cyclopentadienyl ligand substituents. These olefin hydride complexes are potential precursors for the preparation of olefin alkyl complexes. Using these structures as transition state analogues, we hope to gain some insight into the basis of stereoselectivity for propylene polymerizations with group 4 metallocene catalysts.

Results and Discussion

Preparation of Singly [$SiMe_2$]-Bridged Olefin Hydride Complexes. The synthetic strategy for the preparation of group 5 *ansa*-metallocene olefin hydride complexes is based upon the methodology developed for unlinked metallocene complexes. Essential to the synthesis is a convenient route to the corresponding group 5 metallocene dichloride complex, which in turn may be simultaneously reduced and alkylated via addition of an excess of the appropriate Grignard reagent (Scheme 5).

Scheme 5

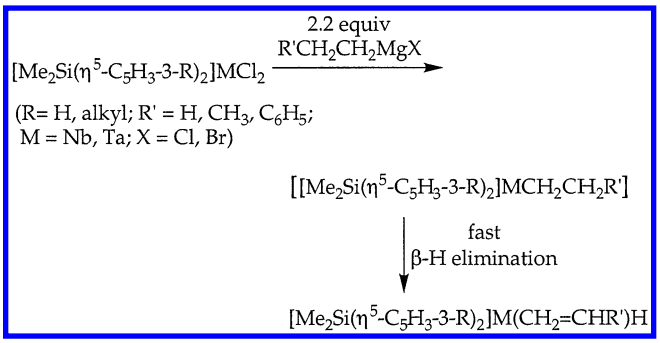

Preparation of *ansa*-niobocene and *ansa*-tantalocene dichloride complexes is accomplished by extension of previously reported synthetic protocols. For the niobocene complexes, metalation of singly [$SiMe_2$]-bridged cyclopentadienyl ligands proceeds via addition of the dilithio salt of the ligand to a slurry of $NbCl_4(THF)_2$ in diethyl ether.[17a] In this manner, [$Me_2Si(\eta^5\text{-}C_5H_4)(\eta^5\text{-}C_5H_3\text{-}3\text{-}CHMe_2)$]$NbCl_2$ (iPrSpNbCl$_2$; **1**), [$Me_2Si(\eta^5\text{-}C_5H_4)(\eta^5\text{-}C_5H_3\text{-}3\text{-}CMe_3)$]$NbCl_2$ (tBuSpNbCl$_2$; **2**), and [$Me_2Si(\eta^5\text{-}C_5H_3\text{-}3\text{-}CMe_3)_2$]$NbCl_2$ (DpNbCl$_2$; **3**) have been prepared (eq 1). Each dichloride complex is first extracted into

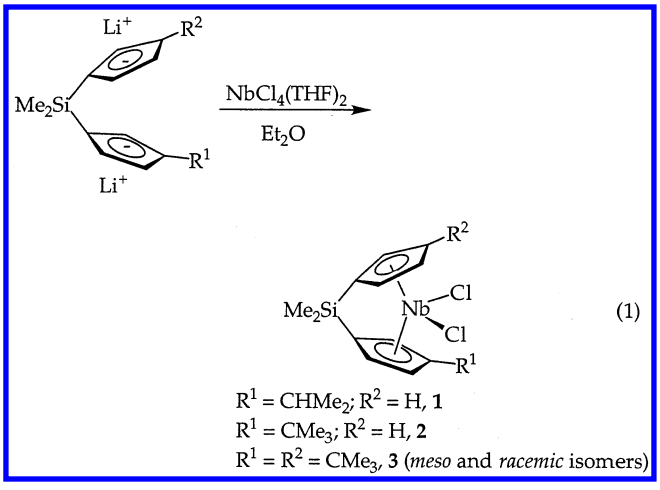

CH_2Cl_2 to remove LiCl. This purification is satisfactory for **1**, but further purification is necessary for **2** and **3**. Complex **2** is isolated after sublimation at 160 °C. Complex **3** is obtained as a mixture of racemic and meso isomers (vide infra), and this mixture is isolated after

(16) (a) Bailey, N. J.; Cooper, J. A.; Gailus, H.; Green, M. L. H.; James, J. T.; Leech, M. A. *J. Chem. Soc., Dalton Trans.* **1997**, 3579. (b) Bailey, N. J.; Green, M. L. H.; Leech, M. A.; Saunders, J. F.; Tidswell, H. M. *J. Organomet. Chem.* **1997**, *538*, 111. (c) Conway, S. L.; Doerrer, L. H.; Green, M. L. H.; Leech, M. A. *Organometallics* **2000**, *19*, 630.

(17) (a) Antiñolo, A.; Martinez-Ripoll, M.; Mugnier, Y.; Otero, A.; Prashar, S.; Rodríguez, A. M. *Organometallics* **1996**, *15*, 3241. (b) García-Yebra, C.; Carrero, F.; López-Mardomingo, C.; Fajardo, M.; Rodríguez, A. M.; Antiñolo, A.; Otero, A.; Lucas, D.; Mugnier, Y. *Organometallics* **1999**, *18*, 1287. (c) Antiñolo, A.; López-Solera, I.; Orive, I.; Otero, A.; Prashar, S.; Rodríguez, A. M.; Villaseñor, E. *Organometallics* **2001**, *20*, 71.

(18) (a) Herrmann, W. A.; Baratta, W. *J. Organomet. Chem.* **1996**, *506*, 357. (b) Herrmann, W. A.; Baratta, W.; Herdtweck, E. *Angew. Chem., Int. Ed. Engl.* **1996**, *35*, 1951.

(19) Chernega, A. N.; Green, M. L. H.; Suárez, A. G. *Can. J. Chem.* **1995**, *73*, 1157.

(20) Shin, J. H.; Parkin, G. *Chem. Commun.* **1999**, 887.

a second extraction into petroleum ether. Characterization of the paramagnetic Nb(IV) dichloride complexes has been accomplished by ambient-temperature EPR spectroscopy and by elemental analysis. The EPR spectra for **1**−**3** display 10-line patterns indicative of a single electron localized on a Nb(IV) center (^{93}Nb = 100%, $S = {}^9/_2$).

Synthesis of the requisite *ansa*-tantalocene complexes follows a different route. Lacking a suitable Ta(IV) precursor, metalation of singly [$SiMe_2$]-bridged cyclopentadienyl ligands is accomplished via reaction of $TaCl_5$ with the corresponding stannylated cyclopentadiene as described previously.[20] In this manner, [$Me_2Si(\eta^5$-$C_5H_4)(\eta^5$-C_5H_3-3-$CHMe_2)$]$TaCl_3$ (iPrSpTaCl_3; **4**), [$Me_2Si(\eta^5$-$C_5H_4)(\eta^5$-C_5H_2-2,4-$(CHMe_2)_2)$]$TaCl_3$ (iPr_2SpTaCl_3; **5**), and [$Me_2Si(\eta^5$-$C_5H_4)(\eta^5$-C_5H_3-3-$CMe_3)$]$TaCl_3$ (tBuSpTaCl_3; **6**) have been prepared in modest yield (eq 2). The diamagnetic Ta(V) trichloride complexes display

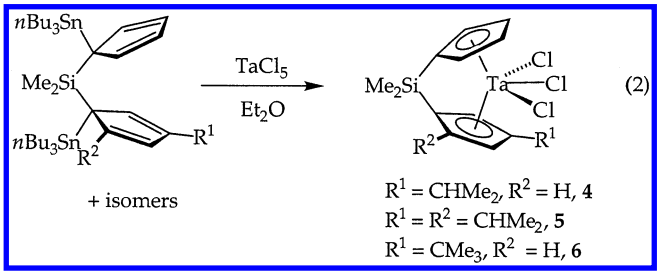

typical ligand resonances in their ^{1}H and ^{13}C NMR spectra (see Experimental Section for details).

Reduction of the orange *ansa*-tantalocene trichloride complexes **4**−**6** with zinc dust in dimethoxyethane affords green iPrSpTaCl_2 (**7**), iPr_2SpTaCl_2 (**8**), and tBuSpTaCl_2 (**9**) in approximately 70% yields (eq 3). The

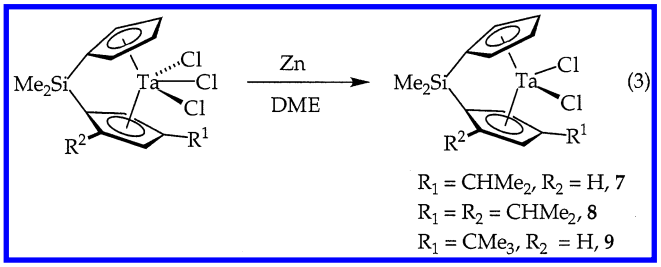

tantalocene dichloride complexes are isolated as forest green solids that are soluble in dimethoxyethane and dichloromethane. Ambient-temperature EPR spectroscopy in dichloromethane solution affords characteristic eight-line spectra (^{181}Ta = 99.99%, $S = {}^7/_2$) consistent with a Ta(IV) d^1 species.

Addition of 2.2 equiv of CH_3CH_2MgBr to either **1** or **7** in diethyl ether results in formation of the ethylene hydride complexes iPrSpM(η^2-CH_2CH_2)H (M = Nb (**10**), Ta (**11**)) (eq 4). For both complexes, ^{1}H NMR spectroscopy reveals that, of the two possible ethylene hydride isomers, one isomer is formed preferentially in a 95:5 ratio. Diagnostic upfield metal hydride resonances are observed at −2.60 and −2.81 ppm for **10** and **11**, respectively. The ^{1}H NMR spectrum for **10** at 25 °C contains broad resonances for the niobium hydride and for the coordinated ethylene, indicative of rapid and reversible olefin insertion and β-hydrogen elimination.[15] When the temperature is lowered to −30 °C, these

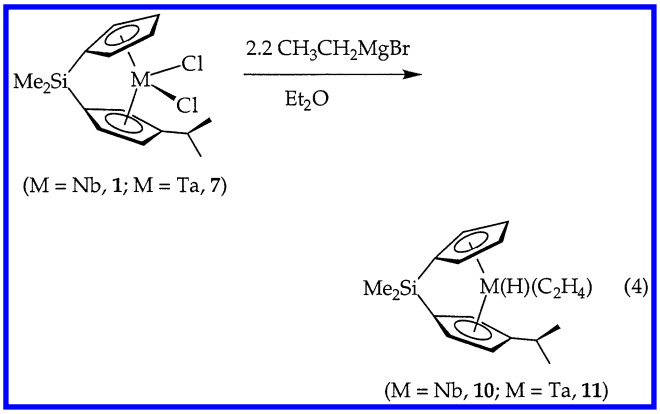

resonances sharpen and are analogous to the (static) 25 °C ^{1}H NMR spectrum for **11**.

Structural assignment of the predominant ethylene hydride isomer for both **10** and **11** has been accomplished with NOE difference NMR spectroscopy.[21] Irradiation of the metal hydride affords a strong NOE enhancement in the isopropyl methine, isopropyl methyl groups, and the *endo*-ethylene protons. Likewise, irradiation of the isopropyl methine results in enhancement in the metal hydride resonance. No enhancement in any ethylene peaks is observed. These data, taken together with more subtle cyclopentadienyl and [$SiMe_2$] NOE enhancements, allow the assignment of the major isomers. In both cases, the ethylene is coordinated in the more open portion of the metallocene wedge, away from the isopropyl substituent (i.e., the distal isomer). The formation of predominantly one ethylene hydride isomer (95%) demonstrates the moderate stereodirecting ability of a monosubstituted *ansa*-metallocene.

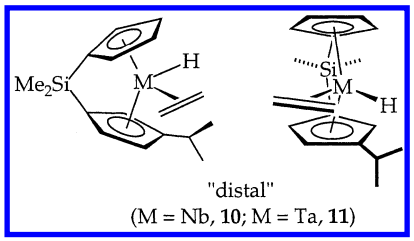

Addition of CH_3CH_2MgBr to either **2** or **9** affords the corresponding *ansa*-niobocene or -tantalocene ethylene hydride complex [$Me_2Si(\eta^5$-$C_5H_4)(\eta^5$-C_5H_3-$CMe_3)M(\eta^2$-$CH_2CH_2)$H] (M = Nb (**12**), Ta (**13**)) in modest yield (eq 5). In both cases only one isomer is observed by ^{1}H NMR spectroscopy. Slow cooling of a petroleum ether solution of **12** affords yellow crystals suitable for X-ray diffraction. The solid-state structure of **12** is shown in Figure 1 and reveals that the ethylene ligand is coordinated in the open portion of the metallocene wedge away from the *tert*-butyl substituent. The niobium hydride was located in a difference map, and the Nb−H bond length was refined to 1.68(2) Å. The C(17)−C(18) bond distance of 1.411(2) Å is consistent with other group 5 olefin adducts, indicative of substantial metallocyclopropane character.[22]

(21) The NOE difference experiment for **10** was performed at −30 °C in order to obtain sharp NMR resonances and reliable structural data.

(22) Guggenberger, L. J.; Meakin, P.; Tebbe, F. N. *J. Am. Chem. Soc.* **1974**, *96*, 5420.

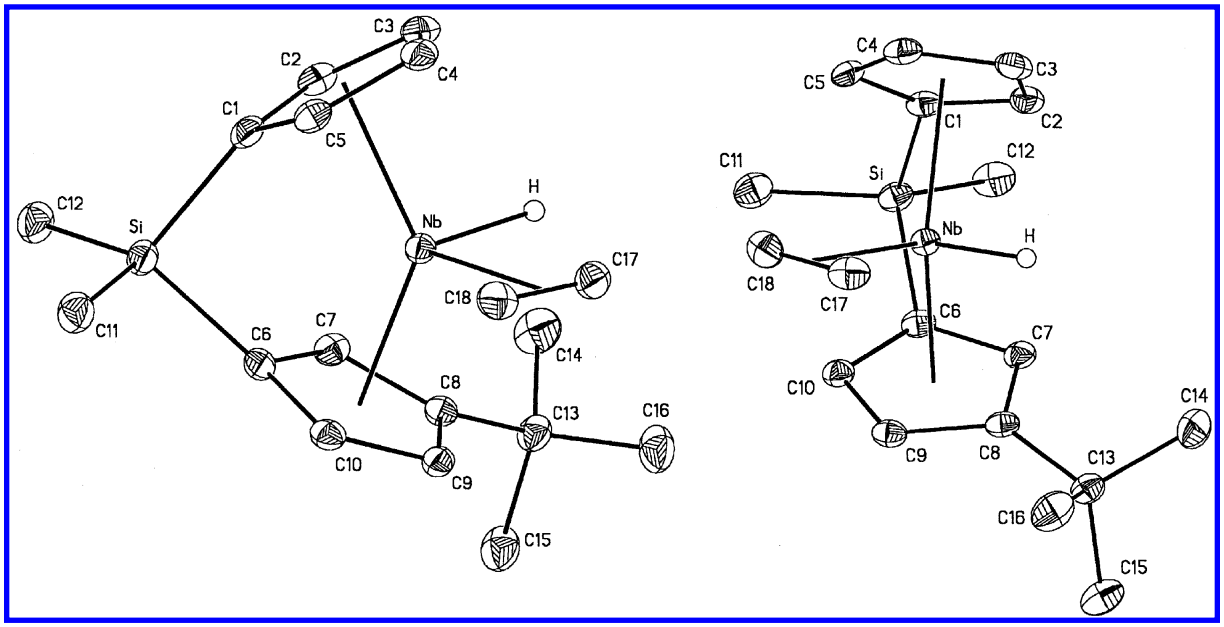

Figure 1. Molecular structure of **12** with 50% probability ellipsoids. Hydrogen atoms (other than hydride shown at arbitrary scale) have been omitted.

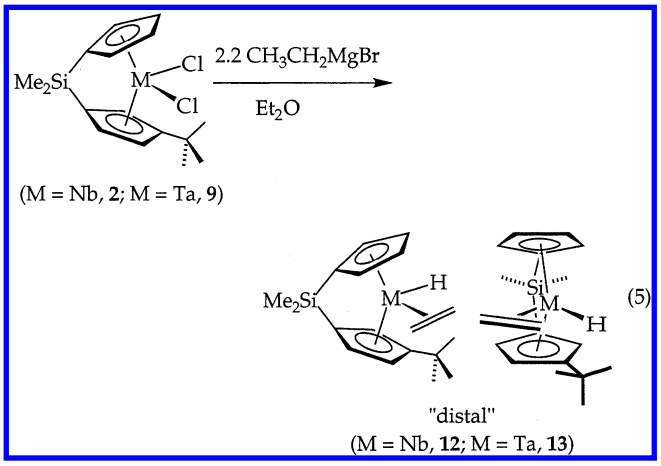

Reaction of the disubstituted *ansa*-tantalocene **8** with CH_3CH_2MgBr affords two isomers of the ethylene hydride complex $iPr_2SpTa(\eta^2\text{-}CH_2CH_2)H$ (**14**) in a 78:22 ratio (eq 6). NOE difference ^1H NMR spectroscopy

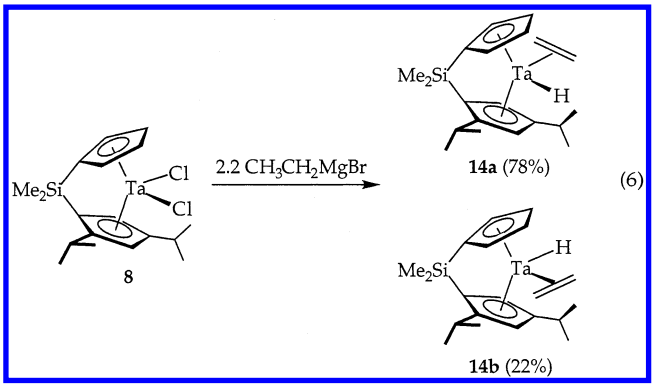

reveals that the ethylene ligand is coordinated on the side of the metallocene wedge proximal to the 4-isopropyl substituent for the major isomer. Although the energy difference between these two isomers is quite small, there does appear to be a slight preference for the olefin to coordinate away from the isopropyl substituent that is α to the linking [$SiMe_2$] group.

Reaction of complex **3** with CH_3CH_2MgBr results in a mixture of two isomers in a 50:50 ratio. The number of cyclopentadienyl resonances in the ^1H NMR indicate that one isomer is of C_s symmetry, *meso*-DpNb(η^2-CH_2-CH_2)H (**15a**); the other isomer, *rac*-DpNb(η^2-CH_2CH_2)H (**15b**), is C_1 symmetric. The isomers, **15a** and **15b**, can be separated by fractional recrystallization from cold petroleum ether. NOE difference experiments for the *meso* isomer **15a** indicate that the ethylene is coordinated away from the *tert*-butyl substituents (eq 7).

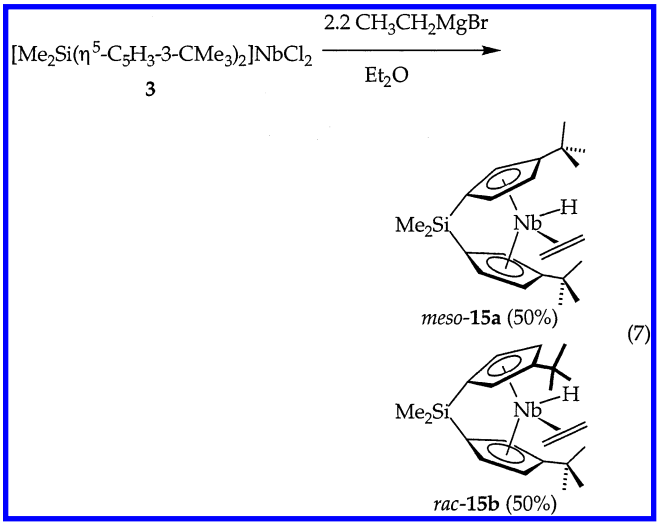

Preparation of *ansa*-niobocene and -tantalocene complexes with α-olefins is accomplished via addition of the appropriate Grignard reagent to the metallocene dichloride complexes. Thus, addition of $CH_3CH_2CH_2MgCl$ to **7** affords a mixture containing four (^1H NMR detectable) isomers of the eight possible for $iPrSpTa(\eta^2\text{-}CH_2\text{-}CHCH_3)H$ (**16**) as a yellow oil with the following percentages: 63.7% (**16a**), 20.6% (**16b**), 13.0% (**16c**), and 2.6% (**16d**). Identification of the major isomer has been achieved using NOE difference NMR spectroscopy. The propylene ligand is coordinated in an distal, endo

fashion with the methyl group directed anti to the cyclopentadienyl substituent.

The preparation of tBuSpTa(η^2-CH_2CHCH_3)H (**17**) has been accomplished in a manner analogous to that for **16**. However, for the more substituted *tert*-butyl derivative, only two isomers of the olefin hydride complex are observed by NMR spectroscopy where the major isomer, **17a**, constitutes 92% of the product mixture. As with **16a**, the structure of **17a** has been elucidated using NOE difference NMR spectroscopy and shown to have the propylene coordinated in the endo arrangement with the propylene directed anti to the cyclopentadienyl substituent.[23]

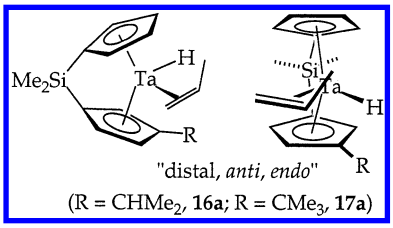

Addition of 2.2 equiv of $C_6H_5CH_2CH_2MgBr$ to an ethereal solution of either **1** or **7** affords the styrene hydride complexes iPrSpM(η^2-$CH_2CHC_6H_5$)H (M = Nb, **18**; Ta, **19**) (eq 8). Three isomers are formed in a 53:

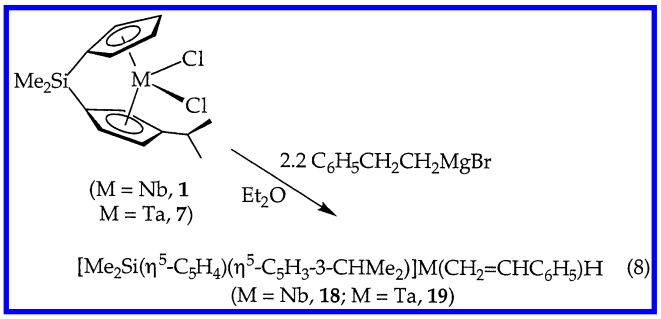

38:9 ratio for **18** and a 54:36:10 ratio for **19** (major: minor:trace isomers).

Analysis of the product mixture by NOE difference ^{1}H NMR spectroscopy allows assignment of the major and minor styrene hydride complexes. Irradiation of the metal hydride resonances results in strong NOE enhancements in the isopropyl substituents, one olefinic styrene resonance, and the ortho hydrogens of the phenyl ring. Likewise, irradiation of the isopropyl substituents results in no enhancement of the styrene protons. These data indicate that for the major isomer of each metal complex, the styrene is coordinated anti to the isopropyl substituents and in endo fashion, where the phenyl ring is directed toward the interior of the metallocene wedge. Presumably unfavorable steric interactions between the phenyl ring and the [Me_2Si] linker discourage formation of exo isomers that were observed with unlinked niobocene and tantalocene styrene hydride complexes.[15a,b]

Differentiation between the enantiofacial preference of styrene hydride isomers has been obtained from more subtle NOE enhancements between the cyclopentadienyl, dimethylsilylene, and styrene hydrogens. For both

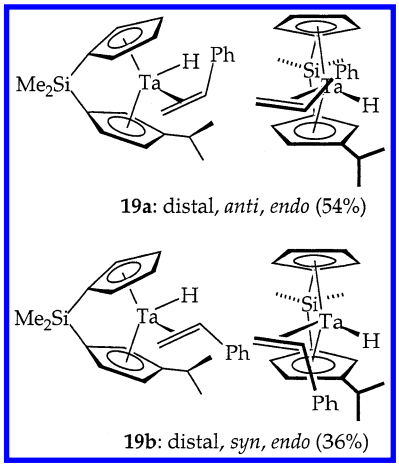

18 and **19** the major styrene hydride isomer is the one for which the phenyl ring is directed away from the isopropyl substituent, whereas in the minor isomer, the phenyl ring is directed toward the isopropyl group, with the diastereoselectivity for olefin coordination for **19** being approximately 18%. A small enantiofacial differentiation was also noted for insertion of 1-pentene into the Y−H bond of a C_2-symmetric yttrocene catalyst and for α-olefin deuteriations.[9,10] Although the enantiofacial preference for olefin coordination is poor, the site selectivity is quite good, where for both **18** and **19** approximately 90% of the styrene coordination occurs with phenyl away from the isopropyl substituent, i.e. "distally".[24]

Slow cooling of a petroleum ether solution of the mixture of isomers of **19** affords yellow needles that are suitable for X-ray diffraction analysis. The solid-state structure for the minor tantalocene styrene hydride complex **19b** reveals the expected η^2 coordination of the styrene ligand. Although the hydride ligand was not located in the difference map, the styrene is bound to the coordination site distal to the isopropyl group (Figure 2). The isopropyl group orients itself such that the methine hydrogen points toward the phenyl group of the coordinated styrene ligand, thus minimizing unfavorable steric interactions between the olefin substituent and the ancillary ligand substitution. The C(16)−C(17) bond distance of 1.420(9) Å is typical for group 5 olefin hydride complexes. The phenyl group on the styrene ligand is twisted 6.2° from the olefin plane (C(16)−C(17)−C(18)), which is reduced substantially from the 32° observed for (η^5-C_5Me_5)$_2$Nb(η^2-CH_2CH-C_6H_5)H.[15b]

Dissolving the single crystals of **19b** in benzene-d_6 reveals that only the minor isomer, **19b**, is initially present. However, over the course of minutes at 25 °C, **19b** isomerizes to the previously observed mixture of products (**19a**:**19b**:**19c** = 54:36:10). The rapid equilibration of the styrene hydride isomers could take place by three possible mechanisms: (a) olefin insertion/β-H elimination, (b) styrene dissociation/recoordination, (c) styrene rotation while coordinated. Because we have independently established that path a is sufficiently rapid to allow rates to be measured by dynamic NMR techniques for niobium and tantalum olefin hydride

(23) The stereoisomer shown (with the *S* metallocene configuration) is one of two mirror-plane-related structures with *si* olefin coordination; the other distal, endo isomer has *re* olefin coordination to the *R* metallocene.

(24) The structure of the isomer comprising 10% of the mixture has not been established, and thus it could be one of the four proximal isomers or one of the two exo distal isomers.

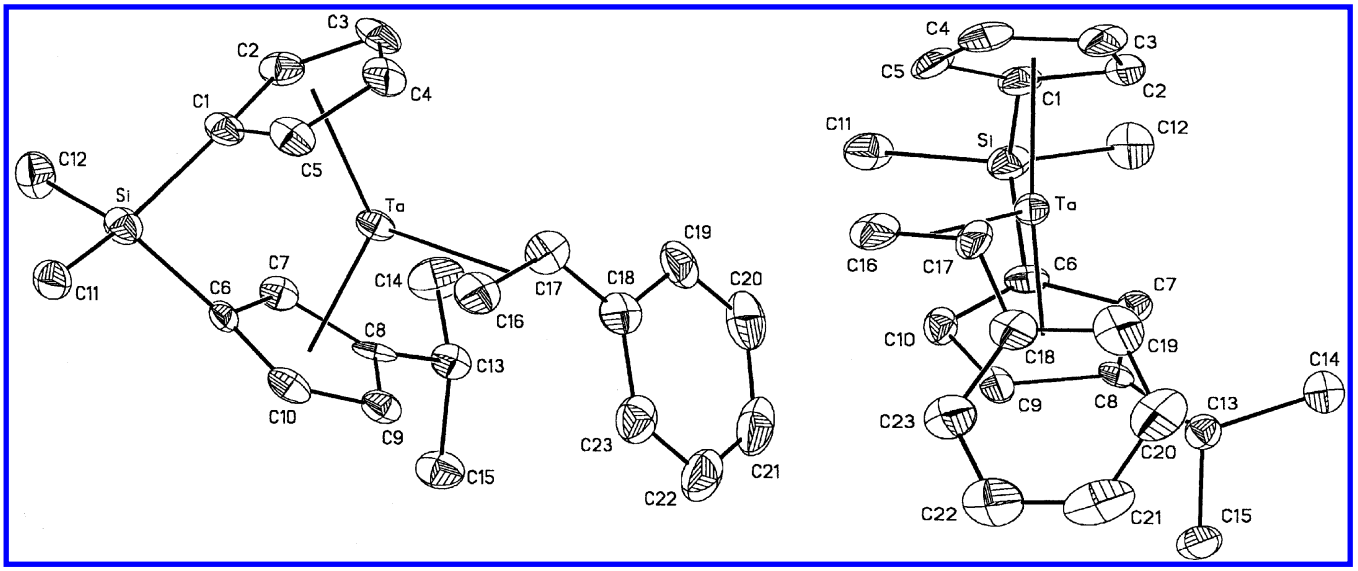

Figure 2. Molecular structure of **19b** with 50% probability ellipsoids. Hydrogen atoms have been omitted.

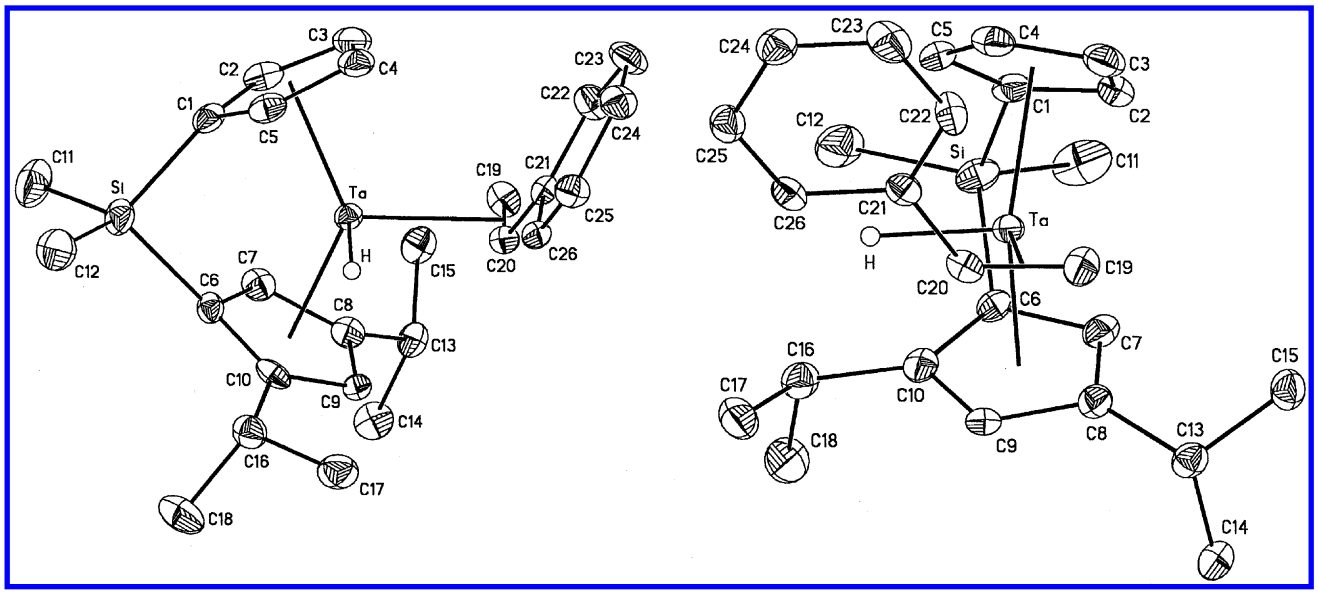

Figure 3. Molecular structure of **20a** with 50% probability ellipsoids. Hydrogen atoms have been omitted except for the hydride, which was located in a difference map but not refined.

complexes, olefin insertion/β-H elimination would appear to be the logical pathway for interconverting **18a** with **18b** and **19a** with **19b**. Styrene dissociation/recoordination, known to be slow for other group 5 olefin hydride complexes,[15a,b] need not be invoked. Indeed, addition of $^{13}CH_2{=}^{13}CH_2$ to a benzene-d_6 solution of **11** results in very slow incorporation of the labeled olefin, requiring 3 days at 25 °C to equilibrate (eq 9). Similarly, addition of ethylene to the isomeric mixture of styrene

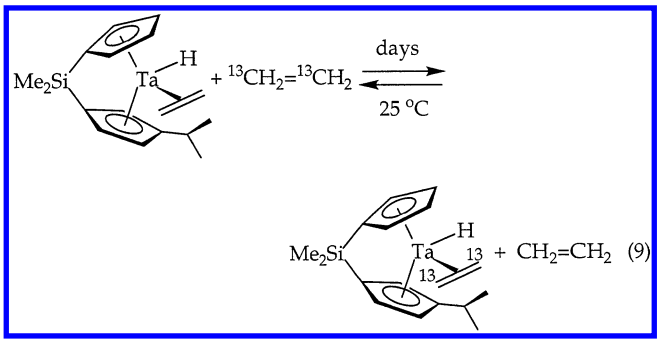

hydride complexes **19a**−**c** results in formation of **11** over the course of 1 week at 23 °C. Thus, a combination of (a) and (c) (Scheme 6) would allow interconversion of all eight possible mirror-plane-related pairs of diastereomers.

Preparation of the styrene hydride complex $iPr_2SpTa(\eta^2\text{-}CH_2CHPh)H$ (**20**) has been accomplished via addition of phenethylmagnesium chloride to a diethyl ether solution of **8** (eq 10). Analysis of the product mixture by ^{1}H NMR spectroscopy indicates that four isomers are formed. The product distribution consists of major and minor isomers formed in a 48:39 ratio constituting 87% of the styrene hydrides. Two trace isomers composing 13% of the product mixture are formed in roughly equal amounts. Recrystallization of the reaction mixture from cold petroleum ether affords yellow needles that are suitable for X-ray diffraction analysis, identifying one isomer (Figure 3). Dissolving the crystals in benzene-d_6 reveals that the isomer that crystallizes is the major isomer formed (**20a**). Monitoring the solution over time by ^{1}H NMR spectroscopy demonstrates that pure **20a**

Scheme 6

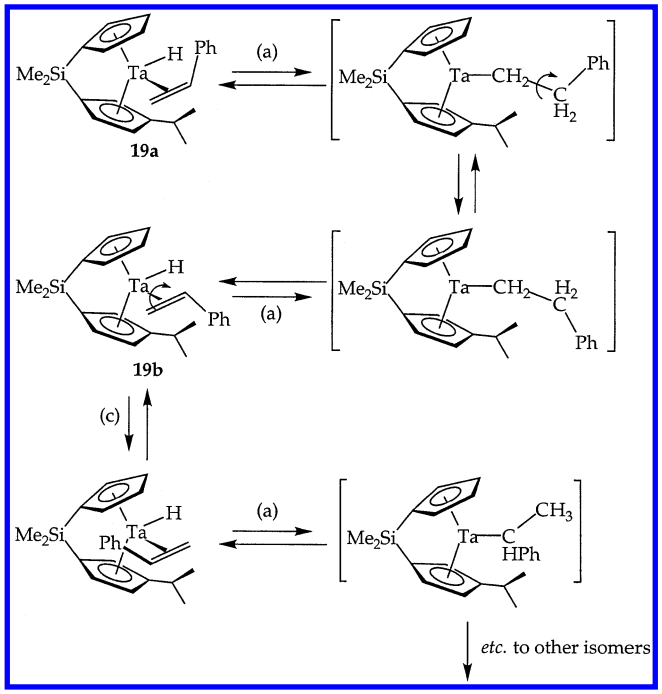

undergoes isomerization (~30 min at 23 °C) to the thermodynamic mixture of styrene hydride products. The major isomer, **20a**, is the one for which the phenyl group of the styrene ligand is directed anti to the isopropyl groups and proximal to the 4-isopropyl substituent, consistent with the major isomer formed in the ethylene hydride complex, **14a** (vide supra), although for **20** the preference is even less.

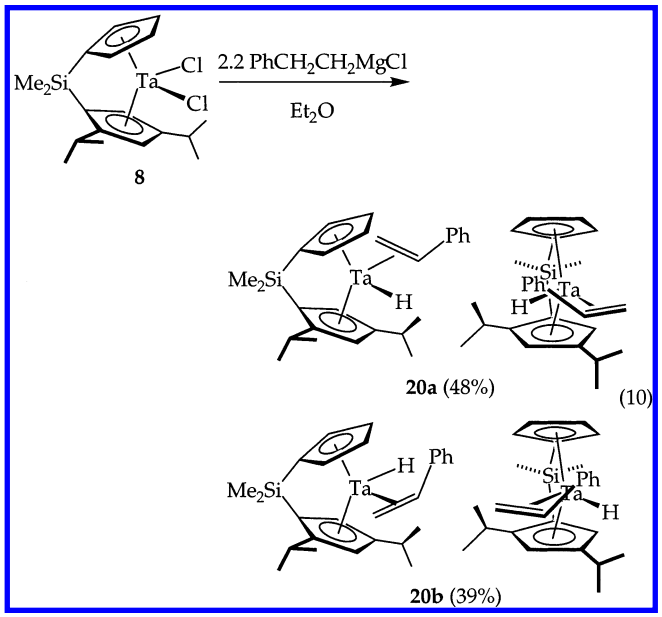

Alkylation of either **2** or **9** with $C_6H_5CH_2CH_2MgCl$ in diethyl ether affords two isomers of tBuSpNb(η^2-CH_2-CHPh)H (**21**) in a 90:10 ratio and only one detectable isomer of tBuSpTa(η^2-CH_2CHPh)H, **22** (eq 11). Slow cooling of a petroleum ether solution of **21** provides yellow crystals (major isomer, **21a**) suitable for X-ray diffraction analysis, as shown in Figure 4. The solid-state structure reveals that the preferred isomer has the styrene coordinated in an endo fashion in the open

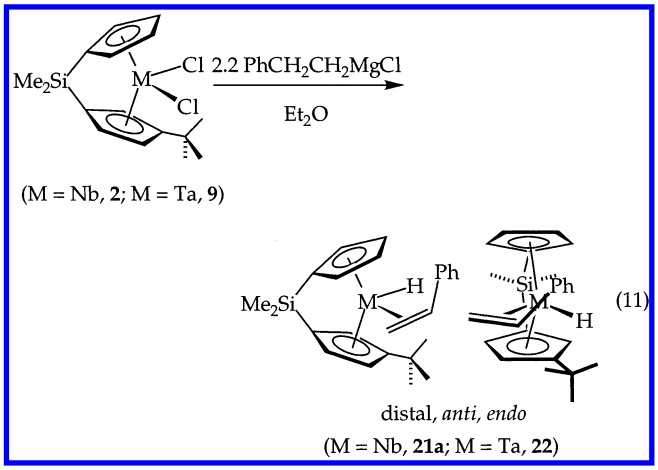

portion of the metallocene wedge with the phenyl group directed anti to the *tert*-butyl substituent. The Nb−H was located in a difference map; the distance was refined to 1.70(2) Å. The phenyl ring exhibits a modest 3.2° twist with respect to the olefinic plane. The C(17)−C(18) bond distance of 1.418(3) Å is similar to that of the complexes described herein and elsewhere.

Slow cooling of a petroleum ether solution of **22** deposits yellow crystals that are suitable for X-ray diffraction analysis. The solid-state structure of **22**, shown in Figure 5, reveals that **22** adopts the geometry of the favored niobium isomer **21a** (the two are isostructural). The hydride ligand was located in the difference map (but not refined) and displays a Ta−H bond length of 1.87 Å. The C(17)−C(18) bond length of 1.445(9) Å and the 4.2° twist to the phenyl ring with respect to the plane of the olefin is consistent with the other *ansa*-tantalocene styrene hydride complexes.

Preparation of Doubly Silylene-Bridged *ansa*-Tantalocene Olefin Hydride Complexes. Reaction of the dipotassio ligand salt K_2[(1,2-$SiMe_2$)$_2$(η^5-C_5H-3,5-($CHMe_2$)$_2$)(η^5-C_5H_2-4-CMe_3)] (K_2tBuThp) with $TaCl_2Me_3$ in benzene-d_6 provides a mixture of two products: [(1,2-$SiMe_2$)$_2$(η^2-C_5H-3,5-($CHMe_2$)$_2$)(η^5-C_5H_2-4-CMe_3)]Ta(CH_3)$_3$ (tBuThpTa(CH_3)$_3$; **23**) and [(1,2-$SiMe_2$)$_2$(η^5-C_5H-3,5-($CHMe_2$)$_2$)(η^5-C_5H_2-4-CMe_3)]Ta(CH_2)CH_3 (tBuThpTa(CH_2)CH_3; **24**) (but in only 24% and 18% yields; eq 12).

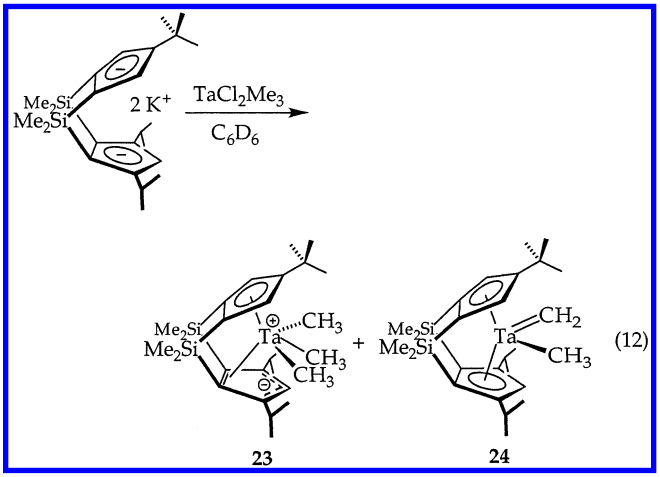

Related *ansa*-tantalocenes with cyclopentadienyl coordination modes analogous to **23** are described elsewhere.[25]

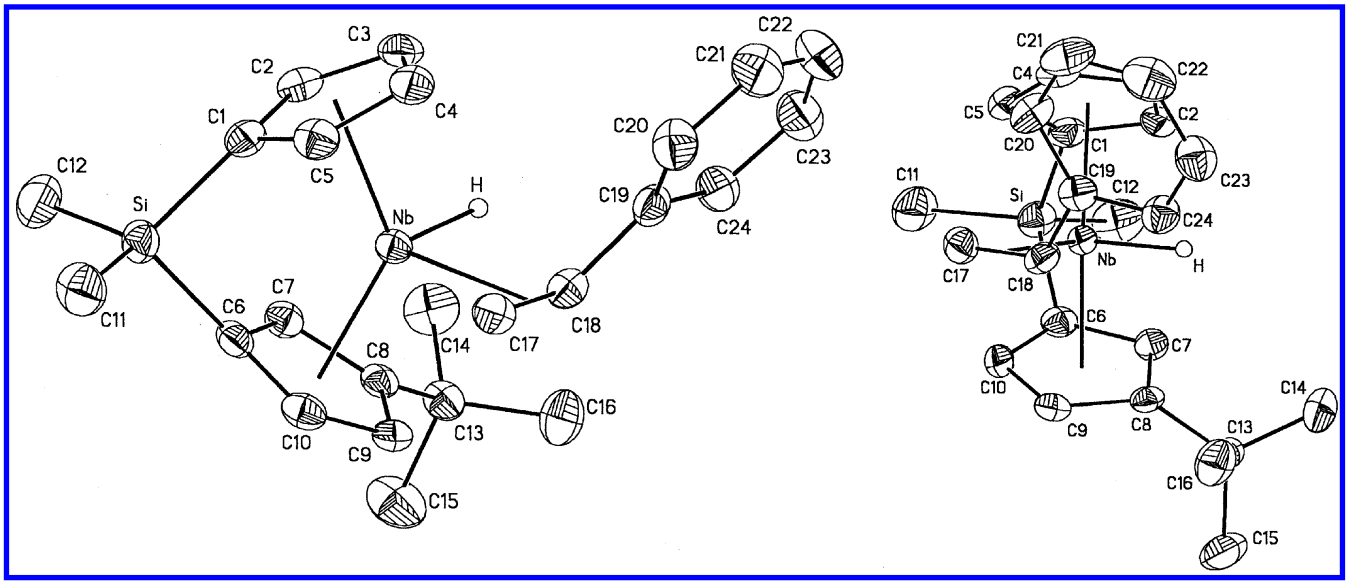

Figure 4. Molecular structure of **21a** with 50% probability ellipsoids. Hydrogen atoms (other than hydride shown at arbitrary scale) have been omitted.

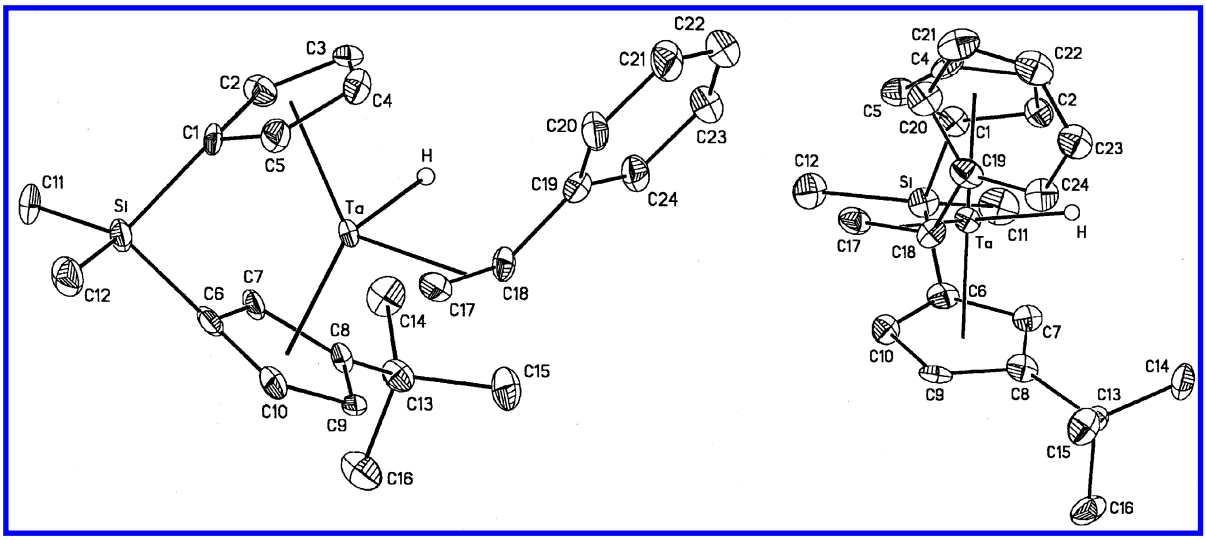

Figure 5. Molecular structure of **22** with 50% probability ellipsoids. Hydrogen atoms have been omitted except for the hydride, which was located in the difference map but not refined.

The mechanism for the formation of **24** is not understood. Interestingly, complex **23** does not appear to be a precursor to **24**; benzene-d_6 solutions of isolated **23** do not provide detectable amounts of **24** over the course of months at 25 °C, whereas heating these solutions leads only to decomposition to other unidentified materials. Moreover, addition of the dipotassio ligand salt K_2tBuThp to solutions of **23** does not lead to **24**, implying that there are two independent pathways for formation of **23** and **24** from $TaCl_2(CH_3)_3$.

The NMR spectral features of the methylene ligand for **24** are most diagnostic of a tantalum alkylidene complex (^{1}H NMR (benzene-d_6), two doublets at δ 9.30 and 9.58; ^{13}C NMR (benzene-d_6), δ 211.3).[26] Slow cooling of a diethyl ether/pentane solution of **24** affords transparent crystals that are suitable for X-ray diffraction.

The solid-state structure of **24**, shown in Figure 6, reveals η^5:η^5 hapticity of the cyclopentadienyl rings. The tantalocene unit sits on a crystallographic mirror plane, and as a consequence the methylidene and methyl substituents are disordered, so that the Ta−C(15) bond distance is 2.154 Å, representing an average of Ta−CH_3 and Ta=CH_2 tantalum−carbon bond lengths.

Much like the (η^5-C_5Me_5)$_2$Ta(CH_2)(CH_3) analogue,[26] thermolysis of **24** at 100 °C in benzene-d_6 over the course of days affords the *ansa*-tantalocene ethylene hydride complex tBuThpTa(η^2-CH_2CH_2)H (**25**), arising from α-migratory insertion of the methyl group into the carbene ligand, followed by β-H elimination (eq 13).

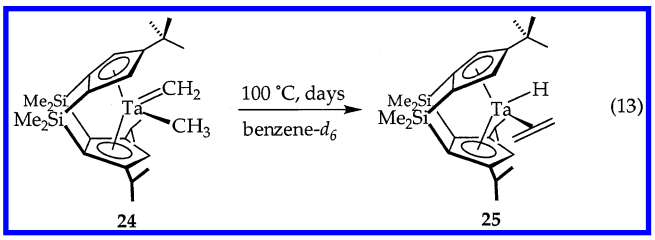

(13)

(25) Chirik, P. J. Ph.D. Thesis, California Institute of Technology, 2000. Zubris, D. L. Ph.D. Thesis, California Institute of Technology, 2001. A drawing and structural details for **23** are included in the Supporting Information.

(26) Parkin, G.; Bunel, E.; Burger, B. J.; Trimmer, M. S.; Asselt, A. V.; Bercaw, J. E. *J. Mol. Catal.* **1987**, *41*, 21.

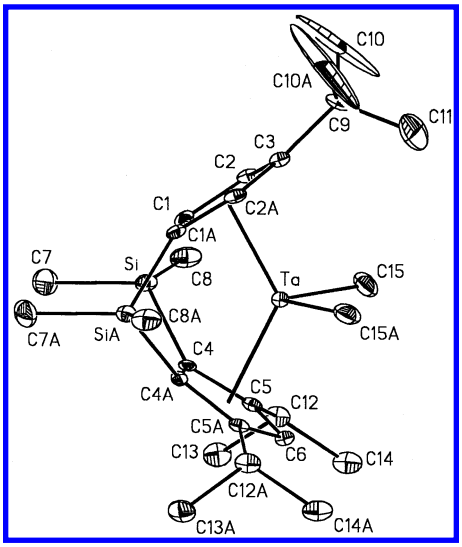

Figure 6. Molecular structure of **24** with 50% probability ellipsoids. Hydrogen atoms have been omitted.

Monitoring the progress of the reaction by ^{1}H NMR spectroscopy reveals the reaction is quantitative and may be carried out on a preparative scale in toluene with only slightly diminished yields.

Addition of excess propylene or styrene to **25** (in separate experiments) results in olefin exchange and formation of the tantalocene propylene hydride or styrene hydride complex tBuThpTa(η^2-CH_2CHR)H (R = CH_3 (**26**), C_6H_5 (**27**)) (eq 14). Although several stereo-

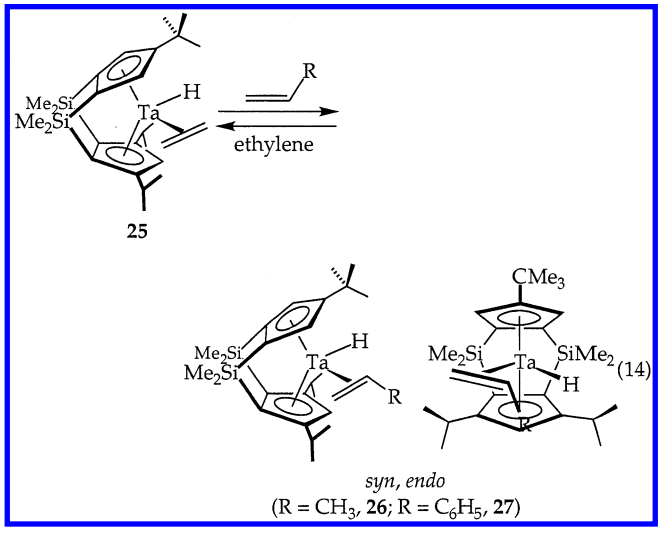

isomers are possible, only two mirror-plane-related diastereomeric tantalocene α-olefin hydride complexes form in NMR-detectable amounts (one is shown in eq 14; syn indicates the relative orientation of the olefin substituents and the isopropyl groups on the cyclopentadienyl ring). NOE difference NMR spectroscopy indicates that the preferred diastereomer has the propylene coordinated in an endo fashion with the propylene methyl group directed away from the bulky *tert*-butyl substituent toward the open region between the isopropyl groups. Unfavorable steric interactions between the propylene methyl group and the dimethylsilylene linkers appear to restrict coordination of the olefin to an endo arrangement. Formation of this diastereomer is consistent with the model previously proposed for this ligand array in the syndiospecific polymerization of propylene.[12,13]

In the case of the styrene hydride complex **27**, three distinct ortho, meta, and para styrene resonances are detected in the ^{1}H NMR spectrum at room temperature, suggesting free rotation about the C−C_{ipso} bond. NOE difference NMR spectroscopy indicates that the preferred isomer is analogous to that for the propylene hydride analogue, i.e. where the olefin is coordinated in an endo arrangement with the phenyl substituent directed between the two isopropyl groups on the cyclopentadienyl ring. It is notable that complexes **26** and **27** exhibit the same thermodynamic preferences for olefin binding despite the increased sterics of bound styrene.

Conclusions

A series of singly [$SiMe_2$]-bridged *ansa*-niobocene and -tantalocene olefin hydride complexes have been prepared via reduction and alkylation of the corresponding niobocene and tantalocene dichloride complexes. Their geometries have been determined in solution by NOE difference NMR spectroscopy, and in several cases the solid-state structures have been established by X-ray diffraction. Monosubstitution of the cyclopentadienyl framework with an isopropyl or *tert*-butyl group ([Me_2-Si(η^5-C_5H_4)(η^5-C_5H_3-3-R)]M(olefin)H; R = $CHMe_2$, CMe_3) directs ethylene coordination such that the olefin is distal from R, ca. 20:1 for isopropyl and >50:1 for *tert*-butyl. The methyl groups of the [$SiMe_2$] linker force α-olefins such as propylene and styrene to coordinate with the olefin substituent directed toward the hydride ligand (endo), unlike the "parent" [(η^5-C_5H_5)$_2$M] olefin hydride complexes, for which approximately equal amounts of endo and exo isomers are obtained for the propylene and styrene hydrides. As for the ethylene hydride complexes, distal coordination of α-olefins is preferred; however, neither isopropyl nor *tert*-butyl substitution of one cyclopentadienyl ligand enforces a strong enantiofacial preference for olefin coordination for the niobium olefin hydrides, although only one mirror-plane-related pair of diastereomers is observed for [Me_2Si(η^5-C_5H_4)(η^5-C_5H_3-3-CMe_3)]Ta(CH_2CHPh)H.

For singly [$SiMe_2$]-bridged *ansa*-tantalocene olefin hydride complexes having 2,4-diisopropyl substitution on one cyclopentadienyl ring ([Me_2Si(η^5-C_5H_4)(η^5-C_5H_2-2,4-($CHMe_2$)$_2$)]Ta(olefin)H), generally lower selectivity for one coordination site over the other is exhibited for ethylene or styrene. Thus, the isopropyl groups appear to work at odds to each other. It is interesting to note that Miya noted lower isospecificity for propylene polymerizations with [Me_2Si(η^5-C_5H_4)(η^5-C_5H_2-2,4-($CHMe_2$)$_2$)]$ZrCl_2$/MAO as compared with [Me_2Si(η^5-C_5H_4)(η^5-C_5H_3-3-$CHMe_2$)]$ZrCl_2$/MAO.[14a] A doubly 1,2-[$SiMe_2$]-bridged *ansa*-tantalocene ethylene hydride complex has been prepared from thermolysis of the corresponding methylidene methyl complex. Addition of propylene or styrene to the ethylene hydride complex results in olefin exchange, affording only one isomer of the α-olefin hydride complex, that with the methyl or phenyl group directed away from the *tert*-butyl substituent and between the isopropyl groups of the other cyclopentadienyl ligand.

Thus, the placement of a single isopropyl or *tert*-butyl substituent on a cyclopentadienyl ligand of [Me_2Si(η^5-

$C_5H_4)(\eta^5$-C_5H_3-3-R)]M(olefin)H has a modest effect in directing the olefin coordination geometry. It would, of course, be of interest to establish the stereodirecting effects of these substituents on the conformations of the M−R′ group for the corresponding [$Me_2Si(\eta^5$-$C_5H_4)(\eta^5$-C_5H_3-3-R)]M(olefin)R′ complexes, particularly for those metal alkyls that mimic the polymeryl groups during propylene polymerization, e.g. [M-$CH_2CH(CH_3)CH_2$-$CHMe_2$], since it has been established that the interactions of the olefin substituents with the polymeryl group are greater than with the ligand substituents (vide supra). Unfortunately, all attempts to induce olefin insertion and olefin coordinative trapping of the resultant alkyls using these *ansa*-olefin hydrides were unsuccessful. Presumably, the equilibrium needed to provide such olefin alkyls (eq 15) lies too far to the left, even for α-olefins.

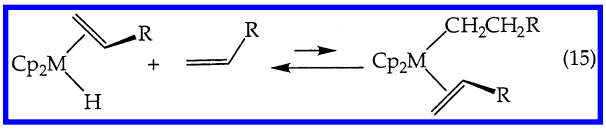

Experimental Section

General Considerations. All air- and moisture-sensitive compounds were manipulated using standard vacuum line, Schlenk, or cannula techniques or in a drybox under a nitrogen atmosphere as described previously.[27] Argon, dinitrogen, and dihydrogen gases were purified by passage over columns of MnO on vermiculite and activated molecular sieves. Toluene and petroleum ether were distilled from sodium and stored under vacuum over titanocene.[28] Tetrahydrofuran, dimethoxyethane, and ether were distilled from sodium benzophenone ketyl. Tetrahydrofuran-d_8 was distilled from sodium benzophenone ketyl and stored over 4 Å molecular sieves. Dichloromethane-d_2 was distilled from CaH_2. $NbCl_4(THF)_2$, $TaCl_5$, (n-$Bu)_3SnCl$, 3.0 M CH_3CH_2MgBr in diethyl ether, 2.0 M $CH_3CH_2CH_2MgCl$ in diethyl ether, and 1.0 M $PhCH_2CH_2MgCl$ in THF were purchased from Aldrich and used as received. Propylene was purchased from Aldrich and dried over $Al(iBu)_3$. Styrene was purchased from Aldrich and distilled from CaH_2 before use. Zinc dust was purchased from Strem Chemical and dried at 100 °C under high vacuum. Ethylene was purchased from Matheson and passed through a dry ice trap immediately before use. All dilithio salts of ligands were prepared according to standard procedures,[29] while $TaCl_2Me_3$ was prepared according to the literature procedure.[30]

NMR spectra were recorded on a JEOL GX-400 (^{1}H, 399.78 MHz; ^{13}C, 100.53 MHz) or a Varian Inova 500 instrument (^{1}H, 500.13 MHz; ^{13}C, 125.77 MHz). All chemical shifts are relative to TMS for ^{1}H (residual) and ^{13}C (solvent as a secondary standard). Nuclear Overhauser difference experiments were carried out on a Varian Inova 500 MHz spectrometer. Elemental analyses were carried out at the Caltech Analytical Facility by Fenton Harvey or by Midwest Microlab, Indianapolis, IN.

[$Me_2Si(\eta^5$-$C_5H_4)(\eta^5$-C_5H_3-3-$CHMe_2)]NbCl_2$ (1). In the drybox, 6.23 g (16.4 mmol) $NbCl_4(THF)_2$ and 4.00 g (16.4 mmol) of $Li_2[Me_2Si(\eta^5$-$C_5H_4)(\eta^5$-C_5H_3-3-$CHMe_2)]$ were combined in a 300 mL round-bottom flask. On the vacuum line, 175 mL Et_2O was added by vacuum transfer. The reaction was stirred overnight. The Et_2O was removed in vacuo leaving a light brown powder. The product was isolated by dissolving the crude mixture in 100 mL of CH_2Cl_2 followed by filtration of the LiCl. The CH_2Cl_2 was removed in vacuo, leaving 5.63 g (87.2%) of a dark brown solid identified as **1**. Anal. Calcd for $NbSiC_{15}H_{20}Cl_2$: C, 46.05; H, 4.90. Found: C, 46.04; H, 4.97. EPR (CH_2Cl_2): $g_{iso} = 2.01$; $a_{iso} = 99.0$ G.

[$Me_2Si(\eta^5$-$C_5H_4)(\eta^5$-C_5H_3-3-$CMe_3)]NbCl_2$ (2). This compound was prepared in a manner analogous to that for **1**, employing 1.00 g (3.91 mmol) of $Li_2[Me_2Si(\eta^5$-$C_5H_4)(\eta^5$-C_5H_3-3-$CMe_3)]$ and 1.48 g of $NbCl_4(THF)_2$ (3.91 mmol), to afford 1.20 g (75.9%) of a dark brown solid identified as **2**. The isolated solid was sublimed, leaving 0.276 g (17.5%) of product. Anal. Calcd for $NbSiC_{16}H_{22}Cl_2$: C, 47.30; H, 5.35. Found: C, 46.88; H, 5.46. EPR (CH_2Cl_2): $g_{iso} = 2.00$; $a_{iso} = 103.8$ G.

[$Me_2Si(\eta^5$-C_5H_3-3-$CMe_3)_2]NbCl_2$ (3). This compound was prepared in a manner analogous to that for **1**, employing 3.00 g (9.60 mmol) of $Li_2[Me_2Si(\eta^5$-C_5H_3-3-$CMe_3)_2]$ and 3.64 g of $NbCl_4(THF)_2$ (9.60 mmol), to afford a dark brown solid identified as **3**. The isolated solid was further purified by extraction into petroleum ether. The solvent was removed, leaving 1.26 g (28.4%) of product. Anal. Calcd for $NbSiC_{20}H_{30}Cl_2$: C, 52.00; H, 6.54. Found: C, 52.42; H, 6.79. EPR (CH_2Cl_2): $g_{iso} = 2.00$; $a_{iso} = 103.8$ G.

[$Me_2Si(C_5H_4)(C_5H_3$-3-$CHMe_2)][Sn(n$-$Bu)_3]_2$. In the drybox, a 100 mL round-bottom flask was charged with 3.50 g (12.3 mmol) of $Li_2[Me_2Si(\eta^5$-$C_5H_4)(\eta^5$-C_5H_3-3-$CHMe_2)]$. The white solid was slurried in 30 mL of Et_2O. Via pipet, 8.32 g (25.2 mmol) of n-Bu_3SnCl was added over the course of 15 min. The reaction flask was then attached to a swivel frit assembly, and the contents were stirred for 3 days at room temperature. The yellow Et_2O solution was filtered and the white precipitate washed with recycled Et_2O. The Et_2O was removed in vacuo, leaving 15.5 g (76.1%) of a yellow oil identified as $[Me_2Si(C_5H_4)$-$(C_5H_3$-3-$CHMe_2)][Sn(n$-$Bu)_3]_2$. ^{1}H NMR (benzene-d_6): δ 0.162 (s, 6H, SiMe_2); 0.760 (t, 7 Hz, 18H, $SnCH_2CH_2CH_2CH_3$); 1.10 (m, 12H, SnBu_3); 1.13 (m, 12H, SnBu_3); 1.41 (m, 12H, SnBu_3); 2.03 (sept, 1H, CHMe$_2$); not located (CHMe_2); 5.13, 5.24, 5.67, 5.96, 6.02, 6.58 (m, 1H, Cp). ^{13}C NMR (benzene-d_6): δ 0.595 (SiMe_2); 12.23 (SnBu_3); 14.37 (SnBu_3); 17.92 (SnBu_3); 28.32 (SnBu_3); 27.68, 29.89 (CHMe_2); 29.78 (CHMe$_2$); 109.96, 114.67, 116.78, 121.59, 124.46, 133.24, 133.46, 3 not located (Cp).

[$Me_2Si(\eta^5$-$C_5H_4)(\eta^5$-C_5H_3-3-$CHMe_2)]TaCl_3$ (4). In the drybox, 4.90 g (6.06 mmol) of $[Me_2Si(C_5H_4)(C_5H_3$-3-$CHMe_2)][Sn$-$(n$-$Bu)_3]_2$ was charged into a 100 mL round-bottom flask and dissolved in approximately 50 mL of Et_2O, forming a clear solution. Small portions of $TaCl_5$ (2.17 g, 6.05 mmol) were then added slowly to the reaction mixture. A red solid forms upon addition of $TaCl_5$. The flask was attached to a swivel frit assembly and the reaction mixture stirred for 12 h. The solid was collected by filtration and was washed with small portions of Et_2O. The red solid was dried in vacuo, yielding 2.00 g (64%) of **4**. ^{1}H NMR (THF-d_8): 0.895 (s, 3H, SiMe_2); 0.961 (s, 3H, SiMe_2); 1.29 (d, 6.5 Hz, 3H, CHMe_2); 1.37 (d, 6.5 Hz, 3H, CHMe_2); 2.87 (sept, 7 Hz, 1H, CHMe$_2$); 6.28, 6.56, 6.97, 7.28, 7.35, 7.61, 7.79 (m, 1H, Cp). ^{13}C NMR: (THF-d_8): δ −5.20 (SiMe_2); −5.48 (SiMe_2); 20.77 (CHMe_2); 24.44 (CHMe_2); 30.52 (CHMe$_2$); 115.34, 116.56, 116.78, 135.42, 138.29, 138.47 (Cp).

[$Me_2Si(C_5H_4)(C_5H_2$-2,4-$(CHMe_2)_2)][Sn(n$-$Bu)_3]_2$. This complex was prepared in a manner analogous to that for $[Me_2Si$-$(C_5H_4)(C_5H_3$-3-$CHMe_2)][Sn(n$-$Bu)_3]_2$ with 3.80 g (13.6 mmol) of $Li_2[Me_2Si(C_5H_4)(C_5H_2$-2,4-$(CHMe_2)_2)]$ and 9.70 g (29.4 mmol) of n-Bu_3SnCl, affording 10.5 g (90.5%) of $[Me_2Si(C_5H_4)(C_5H_2$-2,4-$(CHMe_2)_2)][n$-$Bu_3Sn]_2$. ^{1}H NMR (CD_2Cl_2): δ 0.02 (s, 3H, SiMe_2); 0.30 (s, 3H, SiMe_2); 0.81 (t, 7 Hz, 18H, SnBu_3); 0.89 (t, 7 Hz, 18H, SnBu_3); 1.1−1.6 (m, SnBu_3); 2.60 (sept, 7 Hz, 1H; CHMe$_2$); 2.69 (sept, 7 Hz, 1H; CHMe$_2$); 5.30, 5.55, 5.91, 6.02, 6.10, 1 not located (m, 1H, Cp).

[$Me_2Si(\eta^5$-$C_5H_4)(\eta^5$-C_5H_2-2,4-$(CHMe_2)_2)]TaCl_3$ (5). This complex was prepared in a manner analogous to that for **4** with 6.50 g (7.58 mmol) of $[Me_2Si(\eta^5$-$C_5H_4)(\eta^5$-C_5H_2-2,4-

(27) Burger, B. J.; Bercaw, J. E. In *Experimental Organometallic Chemistry*; Wayda, A. L., Darensbourg, M. Y., Eds.; ACS Symposium Series 357; American Chemical Society: Washington, DC, 1987; Chapter 4.

(28) Marvich, R. H.; Brintzinger, H. H. *J. Am. Chem. Soc.* **1971**, *93*, 2046.

(29) Herzog, T. A. Ph.D. Thesis, California Institute of Technology, 1997.

(30) Schrock, R. R.; Sharp, P. R. *J. Am. Chem. Soc.* **1978**, *100*, 2389.

$(CHMe_2)_2)][Sn(n\text{-}Bu)_3]_2$ and 2.70 g (7.54 mmol) of $TaCl_5$, affording 2.54 g (60%) of **5**. ^{1}H NMR (CD_2Cl_2): δ 0.05 (s, 3H, SiMe_2); 0.30 (s, 3H, SiMe_2); 2.64 (sept; 7 Hz, 1H, CHMe$_2$); 2.72 (sept; 7 Hz, 1H, CHMe$_2$); 5.31, 5.57, 5.92, 6.42, 6.49, 6.58 (m, 1H, Cp). Anal. Calcd for $TaSiC_{18}H_{26}Cl_3$: C, 38.76; H, 4.70. Found: C, 37.96; H, 4.55.

$[Me_2Si(C_5H_4)(C_5H_{3-}3\text{-}CMe_3)][n\text{-}Bu_3Sn]_2$. This complex was prepared in a manner analogous to that for $[Me_2Si(C_5H_4)(C_5H_3\text{-}3\text{-}CHMe_2)][Sn(n\text{-}Bu)_3]_2$ with 3.00 g (11.7 mmol) of $Li_2[Me_2Si(C_5H_4)(C_5H_3\text{-}3\text{-}CMe_3)]$ and 8.10 g (24.5 mmol) of n-Bu_3SnCl, affording 8.73 g (90%) of $[Me_2Si(C_5H_4)(C_5H_3\text{-}3\text{-}CMe_3)][Sn(n\text{-}Bu)_3]_2$. ^{1}H NMR (benzene-$d_6$): δ 0.42 (s, 3H, SiMe_2); 0.45 (s, 3H, SiMe_2); 1.45 (s, 9H, CMe_3); 0.90−1.10, 1.30−1.65 (m, SnBu_3); 5.75, 5.81, 6.24, 6.56, 6.73, 6.88, 6.92 (m, 1H, Cp). ^{13}C NMR (benzene-d_6): δ 11.72, 12.17 (SiMe_2); 30.11 (CMe_3); 154.45 (*C*Me$_3$); 14.26, 17.71, 27.45, 28.00, 28.22, 28.55, 29.85, 32.00 (SnBu_3); 97.54, 98.67, 103.59, 115.63, 121.51, 126.86, 132.29, 132.98, 2 not located (Cp).

$[Me_2Si(\eta^5\text{-}C_5H_4)(\eta^5\text{-}C_5H_3\text{-}3\text{-}CMe_3)]TaCl_3$ (6). This complex was prepared in a manner analogous to that for **4** with 4.55 g (5.47 mmol) of $[Me_2Si(C_5H_4)(C_5H_3\text{-}3\text{-}CMe_3)][Sn(n\text{-}Bu)_3]_2$ and 1.96 g (5.47 mmol) of $TaCl_5$, affording 1.50 g (51.7%) of **6**. ^{1}H NMR (THF-d_8): δ 1.113 (s, 3H, SiMe_2); 1.17 (s, 3H, SiMe_2); 1.40 (s, 9H, CMe_3); 6.23, 6.38, 6.69, 7.27, 7.64, 7.80, 1 not located (s, 1H, Cp). ^{13}C NMR (THF-d_8): −1.68, −0.27 (SiMe_3); 33.34 (CMe_3); 151.71 (*C*Me$_3$); 109.52, 112.83, 118.90, 120.72, 124.61, 131.82, 144.62, 3 not located (Cp). Anal. Calcd for $TaSiC_{16}H_{22}Cl_3$: C, 36.28; H, 4.19. Found: C, 35.75; H, 3.55.

$[Me_2Si(\eta^5\text{-}C_5H_4)(\eta^5\text{-}C_5H_3\text{-}3\text{-}CHMe_2)]TaCl_2$ (7). This compound was prepared in a manner analogous to that for **8**, employing 0.960 g (1.86 mmol) of **4** and 0.121 g (1.86 mmol) of Zn dust, to afford 0.600 g (67.1%) of a green solid identified as **7**. EPR (CH_2Cl_2): $g_{iso} = 1.94$; $a_{iso} = 101.3$ G.

$[Me_2Si(\eta^5\text{-}C_5H_4)(\eta^5\text{-}C_5H_2\text{-}2,4\text{-}(CHMe_2)_2)]TaCl_2$ (8). In the drybox, a fine swivel frit assembly was charged with 2.47 g (4.43 mmol) of **5** and 0.288 g (4.43 mmol) of Zn dust. On the vacuum line, the frit assembly was evacuated and approximately 50 mL of DME was added by vacuum transfer. After 4 h, a forest green reaction mixture formed. After it was stirred for 16 h, the green DME solution was filtered and the remaining solid was washed three times with recycled solvent. The DME was removed in vacuo, leaving an oily green solid. Addition of Et_2O afforded a green precipitate that was collected by filtration and dried in vacuo, leaving 2.20 g (95.1%) of **8**. Sublimation at 140 °C and 10^{-4} Torr affords analytically pure material. Anal. Calcd for $TaSiC_{15}H_{20}Cl_2$: C, 37.51; H, 4.20. Found: C, 37.28; H, 4.23. EPR (CH_2Cl_2): $g_{iso} = 1.94$; $a_{iso} = 92.9$ G.

$[Me_2Si(\eta^5\text{-}C_5H_4)(\eta^5\text{-}C_5H_3\text{-}3\text{-}CMe_3)]TaCl_2$ (9). This compound was prepared in a manner analogous to that for **8**, employing 1.00 g (1.73 mmol) of **6** and 0.115 g (1.73 mmol) of Zn dust, to afford 0.726 g (78.5%) of a green solid identified as **9**. Anal. Calcd for $TaSiC_{16}H_{22}Cl_2$: C, 38.88; H, 4.49. Found: C, 37.55; H, 4.36. EPR (CH_2Cl_2): $g_{iso} = 1.94$; $a_{iso} = 101.2$ G.

$[Me_2Si(\eta^5\text{-}C_5H_4)(\eta^5\text{-}C_5H_2\text{-}3\text{-}CHMe_2)]Nb(\eta^2\text{-}CH_2CH_2)H$ (10a,b). This compound was prepared in a manner analogous to that for **11**, employing 1.50 g (3.824 mmol) of **1** and 3.00 mL (9.0 mmol) of a 3.0 M CH_3CH_2MgBr solution in Et_2O with dimethoxyethane as the solvent. Extraction with petroleum ether followed by slow cooling to −78 °C afforded 0.205 g (15.3%) of an oily yellow solid identified as **10**.

Major Isomer 10a. Yield: 95%. ^{1}H NMR (−30 °C, toluene-d_8): δ −2.60 (s, 1H, Nb−H); 0.16 (s, 3H, SiMe_2); 0.08 (s, 3H, SiMe_2); 0.85 (m, 2H, CH_2=CH_2, exo); 1.22 (d, 7 Hz, 3H, CHMe_2); 1.26 (d, 7 Hz, 3H, CHMe_2); 1.37 (m, 1H, CH_2=CH_2, endo); 1.48 (m, 1H, CH_2=CH_2, endo); 2.81 (sept, 7 Hz, 1H, CHMe$_2$); 3.18, 3.19, 4.24, 4.28, 5.24, 5.26, 5.80 (m, 1H, Cp). ^{13}C NMR (benzene-d_6): δ −6.79 (SiMe_2); −4.19 (SiMe_2); 11.25 (*C*H$_2$=CH_2, endo); 20.54 (*C*H$_2$=CH_2, exo); 23.93 (CHMe_2); 24.52 (CHMe_2); 28.96 (*C*HMe$_2$); 70.56, 71.97, 82.94, 84.66, 91.71, 93.00, 103.30, 104.65, 106.23, 136.86 (Cp).

Minor Isomer 10b. Yield: 5%. ^{1}H NMR (−30 °C, toluene-d_8): δ −2.69 (s, 1H, Nb−H); 0.13 (s, 3H, SiMe_2); not located (s, 3H, SiMe_2); 0.96 (m, 2H, CH_2=CH_2, exo); 1.57 (m, 2H, CH_2=CH_2, endo); 2 not located (CHMe_2); 2.67 (m, 1H, CHMe$_2$); 3.43, 5.03 (2H), 5.53, 5.76, 2 not located (m, 1H, Cp). ^{13}C NMR (benzene-d_6): δ −6.53 (SiMe_2); −4.49 (SiMe_2); 12.88 (*C*H$_2$=CH_2, endo); 18.27 (*C*H$_2$=CH_2, exo); 21.58 (CHMe_2); 25.77 (CHMe_2); 31.72 (*C*HMe$_2$); 85.01, 85.22, 93.29, 100.13, 102.26, 105.70, 4 not located (Cp).

$[Me_2Si(\eta^5\text{-}C_5H_4)(\eta^5\text{-}C_5H_3\text{-}3\text{-}CHMe_2)]Ta(\eta^2\text{-}CH_2CH_2)H$ (11). In the drybox, a fine swivel frit assembly was charged with 0.300 g (0.625 mmol) of **7**. On the vacuum line, approximately 25 mL of Et_2O was added by vacuum transfer. At −80 °C, against an Ar counterflow, 1.00 mL (3.0 mmol) of a 3.0 M CH_3CH_2MgBr solution was added by syringe. The reaction mixture was stirred and slowly warmed to room temperature. After 2 h, an orange solution and brown precipitate form. The reaction mixture was stirred for 16 h, after which time the Et_2O was removed and replaced with 10 mL of petroleum ether. The product was extracted several times with petroleum ether. The solvent was removed in vacuo, leaving a yellow oil identified as **11**. ^{1}H NMR (benzene-d_6): δ −2.81 (s, 1H, Ta−H); 0.16 (s, 3H, SiMe_2); 0.29 (s, 3H, SiMe_2); 0.90 (m, 2H, CH_2=CH_2, endo); 0.93 (m, 2H, CH_2=CH_2, exo); 1.04 (s, 9H, CMe_3); 3.21, 3.23, 4.14, 4.22, 5.38 (2H), 5.97 (m, 1H, Cp). ^{13}C NMR (benzene-d_6): δ −6.23 (SiMe_2); −3.14 (SiMe_2); 2.44 (*C*H$_2$=CH_2, endo); 14.33 (*C*H$_2$=CH_2, exo); 32.36 (CMe_3); 143.78 (*C*Me$_3$); 79.54, 82.27, 92.55, 94.03, 100.94, 103.79, 105.28, 3 not located (Cp).

$[Me_2Si(\eta^5\text{-}C_5H_4)(\eta^5\text{-}C_5H_3\text{-}3\text{-}CMe_3)]Nb(\eta^2\text{-}CH_2CH_2)H$ (12). This compound was prepared in a manner similar to that for **11**, employing 0.180 g (0.444 mmol) of **2** and 326 μL (0.98 mmol) of a 3.0 M CH_3CH_2MgBr solution in Et_2O. Extraction with petroleum ether followed by slow cooling to −40 °C afforded 0.044 g (27%) of a yellow crystalline solid identified as **12**. ^{1}H NMR (benzene-d_6): δ −2.56 (s, 1H, Nb−H); 0.10 (s, 3H, SiMe_2); 0.19 (s, 3H, SiMe_2); 0.91 (m, 2H, CH_2=CH_2, exo); 1.33 (s, 9H, CMe_3); 1.42 (m, 2H, CH_2=CH_2, endo); 3.16, 3.19, 4.19, 4.25, 5.27 (2H), 5.86 (m, 1H, Cp). ^{13}C NMR (benzene-d_6): δ −6.94 (SiMe_2); −4.04 (SiMe_2); 11.17 (*C*H$_2$=CH_2, endo); 21.51 (*C*H$_2$=CH_2, exo); 31.85 (*C*Me$_3$); 32.00 (CMe_3); 70.18, 71.62, 81.22, 83.97, 92.09, 93.60, 102.55, 103.58, 105.46, 142.81 (Cp).

$[Me_2Si(\eta^5\text{-}C_5H_4)(\eta^5\text{-}C_5H_3\text{-}3\text{-}CMe_3)]Ta(\eta^2\text{-}CH_2CH_2)H$ (13). This compound was prepared in a manner similar to that for **11**, employing 0.400 g (0.833 mmol) of **9** and 0.610 mL (1.8 mmol) of a 3.0 M CH_3CH_2MgBr solution in diethyl ether. Extraction with petroleum ether afforded 0.245 g (69.5%) of a yellow oil identified as **13**. ^{1}H NMR (benzene-d_6): δ −2.72 (s, 1H, Ta−H); 0.19 (s, 3H, SiMe_2); 0.30 (s, 3H, SiMe_2); 0.51 (m, 2H, CH_2=CH_2, endo); 1.10 (m, 2H, CH_2=CH_2, exo); 1.23 (d, 7 Hz, 3H, CHMe_2); 1.29 (d, 7 Hz, 3H, CHMe_2); 2.90 (sept, 7 Hz, 1H, CHMe$_2$); 3.40, 4.32, 4.42, 4.47, 5.35 (2H), 5.94 (m, 1H, Cp). ^{13}C NMR (benzene-d_6): δ −6.92 (SiMe_2); −4.10 (SiMe_2); 11.87 (*C*H$_2$=CH_2, endo); 30.10 (*C*H$_2$=CH_2, exo); 23.65 (CHMe_2); 25.73 (CHMe_2); 28.45 (*C*HMe$_2$); 80.62, 82.38, 91.90, 93.26 102.10, 104.05, 105.49, 3 not located (Cp).

$[Me_2Si(\eta^5\text{-}C_5H_4)(\eta^5\text{-}C_5H_{2-}2,4\text{-}(CHMe_2)_2)]Ta(\eta^2\text{-}CH_2\text{-}CH_2)H$ (14a,b). This compound was prepared in a manner similar to that for **11**, employing 0.340 g (0.651 mmol) of **8** and 0.477 mL (1.4 mmol) of a 3.0 M CH_3CH_2MgBr solution in diethyl ether. Extraction with petroleum ether afforded **14** as a yellow oil.

Major Isomer 14a. Yield: 78%. ^{1}H NMR (benzene-d_6): δ −2.69 (s, 1H, Ta−H); 0.15 (s, 3H, SiMe_2); 0.29 (s, 3H, SiMe_2); 0.42 (m, 2H, CH_2=CH_2, endo); 0.89 (m, 2H, CH_2=CH_2, exo); 0.95 (d, 7 Hz, 3H, CHMe_2); 0.92 (d, 7 Hz, 3H, CHMe_2); 1.26 (d, 7 Hz, 3H, CHMe_2); 1.36 (d, 7 Hz, 3H, CHMe_2); 2.78 (sept, 7 Hz, 1H, CHMe$_2$); 2.47 (sept, 7 Hz, 1H, CHMe$_2$); 3.88, 4.45, 4.97, 5.02, 5.26, 5.41. ^{13}C NMR: (benzene-d_6): δ −1.86 (SiMe_2); 1.36 (SiMe_2); 30.55 (CH_2=CH_2, exo); 8.80 (CH_2=CH_2, endo); 20.88 (CMe_2); 22.72 (CMe_2); 27.71 (CMe_2); 13.90 (CMe_2); 29.70 (*C*Me$_2$);

30.18 (*C*Me_2); 89.57, 92.60, 96.61, 102.03, 104.22, 123.89, 125.99, *3* not located (Cp).

Minor Isomer 14b. Yield: 22%. ^{1}H NMR (benzene-d_6): δ −2.78 (s, 1H, Ta−*H*); 0.17 (s, 3H, Si*Me*$_2$); 0.30 (s, 3H, Si*Me*$_2$); 0.25 (m, 2H, CH_2═CH_2, endo); 0.76 (m, 2H, CH_2═CH_2, exo); 0.97 (d, 7 Hz, 3H, CH*Me*$_2$); 1.30 (d, 7 Hz, 3H, CH*Me*$_2$); 2 not located (CH*Me*$_2$); 2.04 (sept, 7 Hz, 1H, C*H*Me_2); 2.23 (sept, 7 Hz, 1H, C*H*Me_2); 4.26, 4.33, 4.78, 5.80, 5.10, 5.21. ^{13}C NMR (benzene-d_6): δ −4.63 (Si*Me*$_2$); 1.14 (Si*Me*$_2$); 30.61 (*C*H_2═CH_2, exo); 10.72 (*C*H_2═CH_2, endo); 11.31 (C*Me*$_2$); 16.52 (C*Me*$_2$); 18.62 (C*Me*$_2$); not located (C*Me*$_2$); 26.29 (*C*Me_2); not located (*C*Me_2); 91.12, 94.08, 95.16, 100.82, 100.91, 123.60, 125.73, 3 not located (Cp).

[Me_2Si(η^5-C_5H_3-3-CMe_3)$_2$]Nb(η^2-CH_2CH_2)H (15a,b). This compound was prepared in a manner similar to **11** by employing 0.286 g (0.619 mmol) of **3** and 0.480 mL (1.4 mmol) of a 3.0 M CH_3CH_2MgBr solution in Et_2O. Extraction with petroleum ether followed by slow cooling to −40 °C afforded a yellow crystalline solid identified as the *meso* isomer. Subsequent fractional recrystallization allows separation of *rac* and *meso* isomers (0.030 g *meso* isomer isolated; 12% of total yield). The *rac* isomer is isolated as an orange oil.

***meso* Isomer 15a.** Yield: 50%. ^{1}H NMR (500 MHz, toluene-d_8): δ −2.70 (s, 1H, Nb−*H*); 0.15 (s, 3H, Si*Me*$_2$); 0.21 (s, 3H, Si*Me*$_2$); 0.87 (m, 2H, CH_2═CH_2, exo); 1.28 (s, 18H, C*Me*$_3$); 1.37 (m, 2H, CH_2═CH_2, endo); 3.16, 4.28, 5.26 (m, 2H, Cp). ^{13}C NMR (300 MHz, toluene-d_8): δ −6.91 (Si*Me*$_2$); −3.73 (Si*Me*$_2$); 12.57 (*C*H_2═CH_2, endo); 22.60 (*C*H_2═CH_2, exo); 26.16 (*C*Me_3); 32.14 (C*Me*$_3$); 69.64, 81.19, 92.99, 102.13, 143.10 (Cp).

***rac* Isomer 15b.** Yield: 50%. ^{1}H NMR (300 MHz, toluene-d_8): δ −2.39 (s, 1H, Nb−*H*); 0.18 (s, 3H, Si*Me*$_2$); 0.25 (s, 3H, Si*Me*$_2$); not located (CH_2═CH_2, exo); 0.89 (s, 9H, C*Me*$_3$); not located (CH_2═CH_2, endo); 1.29 (s, 9H, C*Me*$_3$); 3.15, 4.24, 4.27, 5.25, 5.34, 5.89 (m, 1H, Cp). ^{13}C NMR (500 MHz, toluene-d_8): δ −6.84 (Si*Me*$_2$); −3.33 (Si*Me*$_2$); 11.10 (*C*H_2═CH_2, endo); 17.85 (*C*H_2═CH_2, exo); 30.60, 32.07 (C*Me*$_3$); not located (*C*Me_3); 69.97, 72.42, 81.38, 85.96, 91.70, 95.65, 102.06, 102.43, 130.65, 142.87 (Cp).

[Me_2Si(η^5-C_5H_4)(η^5-C_5H_3-3-$CHMe_2$)]Ta(η^2-CH_2CH-CH_3)H (16a,b). In the drybox, a fine swivel frit assembly was charged with 0.225 g (0.514 mmol) of **7**. On the vacuum line, approximately 25 mL of Et_2O was added by vacuum transfer. At −80 °C, against an Ar counterflow, 0.56 mL (1.1 mmol) of a 2.0 M $CH_3CH_2CH_2MgCl$ solution in diethyl ether was added via syringe. The reaction mixture was stirred and slowly warmed to room temperature. With warming an orange solution and brown precipitate form. The reaction mixture was stirred for 24 h, and the Et_2O was removed in vacuo and replaced with petroleum ether. The product was extracted several times with petroleum ether. The solvent was removed in vacuo, leaving a thick orange oil identified as **16**.

Major Isomer 16a. Yield: 64%. ^{1}H NMR (benzene-d_6): δ −2.71 (s, 1H, Ta−*H*); 0.04 (s, 3H, Si*Me*$_2$); 0.12 (s, 3H, Si*Me*$_2$); 1.23 (d, 7 Hz, 3H; CH*Me*$_2$); 1.30 (d, 7 Hz, 3H, CH*Me*$_2$); 2.89 (sept, 6.5 Hz, 1H, C*H*Me_2); 0.44 (dd, 10 Hz, 6 Hz, 1H, CH_2═$CHCH_3$); 0.87 (dd, 10 Hz, 6 Hz, 1H CH_2═$CHCH_3$); 1.01 (m, 1H, CH_2═C*H*CH_3); 2.21 (d, 6.5 Hz, 3H, CH_2═CHC*H*$_3$); 3.37, 3.79, 4.40, 4.56, 5.15, 5.57, 5.59 (m, 1H, Cp). ^{13}C NMR (benzene-d_6): δ −6.63 (Si*Me*$_2$); −4.27 (Si*Me*$_2$); 30.17 (*C*H_2═$CHCH_3$); 28.77 (CH_2═*C*HCH_3); 24.23 (CH_2═CH*C*H_3); 21.63 (CH*Me*$_2$); 21.76 (CH*Me*$_2$); 29.03 (*C*HMe_2); 81.62, 83.10, 81.31, 91.39, 104.37, 106.70, 106.81, 3 not located (Cp).

Minor Isomer 16b. Yield: 21%. ^{1}H NMR (benzene-d_6): δ −2.65 (s, 1H, Ta−*H*); 0.10 (s, 3H, Si*Me*$_2$); 0.15 (s, 3H, Si*Me*$_2$); 1.25 (d, 7 Hz, 3H, CH*Me*$_2$); 1.27 (d, 7 Hz, 3H, CH*Me*$_2$); 2.80 (sept, 6.5 Hz, 1H, C*H*Me_2); 3 propylene resonances not located; 2.25 (d, 6.5 Hz, 3H, CH_2═CHC*H*$_3$); 3.30, 3.65, 4.36, 4.37, 5.18, 5.36, 5.91 (m, 1H, Cp). ^{13}C NMR (benzene-d_6): δ −7.01 (Si*Me*$_2$); −3.44 (Si*Me*$_2$); 29.69 (*C*H_2═$CHCH_3$); 23.85 (CH_2═*C*HCH_3); 25.98 (CH_2═CH*C*H_3); 21.28 (CH*Me*$_2$); 22.52 (CH*Me*$_2$); 27.76 (*C*HMe_2); 79.50, 84.81, 91.02, 94.26, 98.10, 99.34, 107.38, 3 not located (Cp).

[Me_2Si(η^5-C_5H_4)(η^5-C_5H_3-3-CMe_3)]Ta(η^2-CH_2CHCH_3)H (17a). This compound was prepared in a manner similar to that for **16**, employing 0.500 g (0.935 mmol) of **9** and 1.05 mL (2.1 mmol) of 2.0 M $CH_3CH_2CH_2MgCl$ solution, to yield 0.220 g (46.5%) of a yellow oil identified as **17**. ^{1}H NMR (benzene-d_6): δ −2.88 (s, 1H, Ta−*H*); 0.02 (s, 3H, Si*Me*$_2$); 0.09 (s, 3H, Si*Me*$_2$); 1.30 (s, 9H, C*Me*$_3$); 0.44 (dd, 10 Hz, 6 Hz, 1H, CH_2═$CHCH_3$); 0.89 (dd, 10 Hz, 6 Hz, 1H, CH_2═$CHCH_3$); 1.02 (m, 1H, CH_2═C*H*CH_3); 2.17 (d, 6.5 Hz, 3H, CH_2═CHC*H*$_3$); 3.24, 3.63, 4.23, 4.56, 5.11, 5.59, 5.62 (m, 1H, Cp). ^{13}C NMR (benzene-d_6): δ −6.32 (Si*Me*$_2$); −4.01 (Si*Me*$_2$); 28.18 (*C*H_2═$CHCH_3$); 28.98 (CH_2═*C*HCH_3); 23.19 (CH_2═CH*C*H_3); 32.23 (C*Me*$_3$); 142.46 (C*Me*$_3$); 80.37, 82.53, 92.42, 92.94, 103.91, 105.23, 105.58, 3 not located (Cp).

[Me_2Si(η^5-C_5H_4)(η^5-C_5H_3-3-$CHMe_2$)]Nb(η^2-CH_2CHPh)H (18a−c). This compound was prepared in a manner similar to that for **11**, employing 2.00 g (5.09 mmol) of **1** and 12 mL (12 mmol) of a 1.0 M $PhCH_2CH_2MgCl$ solution in THF. Extraction with petroleum ether followed by removal of the solvent in vacuo afforded 0.325 g (15.0%) of an oily yellow solid identified as **18**.

Major Isomer 18a. Yield: 53%. ^{1}H NMR (benzene-d_6): δ −1.96 (s, 1H, Nb−*H*); −0.04 (s, 3H, Si*Me*$_2$); 0.08 (s, 3H, Si*Me*$_2$); 1.07 (dd, 10 Hz, 5 Hz, 1H, CH_2═CHPh, trans); 1.21 (d, 7 Hz, 3H, CH*Me*$_2$); 1.32 (d, 7 Hz, 3H, CH*Me*$_2$); 1.46 (dd, 13 Hz, 5 Hz, 1H, CH_2═CHPh, cis); 2.80 (sept, 7 Hz, 1H, C*H*Me_2); 3.50 (m, 1H, CH_2═C*H*Ph); 3.58, 3.60, 4.35, 4.38, 4.96, 5.14, 5.49 (m, 1H, Cp). ^{13}C NMR (benzene-d_6): δ −6.04 (Si*Me*$_2$); −3.94 (Si*Me*$_2$); 19.96 (*C*H_2═CHPh); 24.77 (CH*Me*$_2$); 25.15 (CH*Me*$_2$); 29.67 (*C*HMe_2); 39.43 (CH_2═*C*HPh); 73.63, 75.06, 85.55, 88.63, 94.21, 96.06, 105.15, 108.73, 113.36, 136.53 (Cp); 122.49 (C_6H_5, para); not located (C_6H_5, ortho); 128.20 (C_6H_5, meta); 153.23 (C_6H_5, ipso).

Minor Isomer 18b. Yield: 38%. ^{1}H NMR (benzene-d_6): δ −2.15 (s, 1H, Nb−*H*); −0.02 (s, 3H, Si*Me*$_2$); 0.09 (s, 3H, Si*Me*$_2$); 0.74 (d, 7 Hz, 3H, CH*Me*$_2$); 1.12 (dd, 10 Hz, 5 Hz, 1H, CH_2═CHPh, trans); 1.23 (d, 7 Hz, 3H, CH*Me*$_2$); 1.36 (dd, 13 Hz, 5 Hz, 1H, CH_2═CHPh, cis); 1.52 (sept, 7 Hz, 1H, C*H*Me_2); 3.50 (m, 1H, CH_2═C*H*Ph); 3.42, 3.45, 4.27, 4.30, 5.19, 5.55, 5.95 (m, 1H, Cp). ^{13}C NMR (benzene-d_6): δ −6.24 (Si*Me*$_2$); −3.67 (Si*Me*$_2$); 20.63 (*C*H_2═CHPh); 22.53 (*C*HMe_2); 26.43 (CH*Me*$_2$); 26.79 (CH*Me*$_2$); 37.93 (CH_2═*C*HPh); 73.83, 75.04, 82.96, 86.81, 95.31, 96.15, 104.16, 110.15, 113.34, 138.34 (Cp); 122.15 (C_6H_5, para); 127.45 (C_6H_5, ortho); not located (C_6H_5, meta); 152.95 (C_6H_5, ipso).

Trace Isomer 18c. Yield: 9%. ^{1}H NMR (benzene-d_6): δ −2.09 (s, 1H, Nb−*H*); −0.05 (s, 3H, Si*Me*$_2$); 0.06 (s, 3H, Si*Me*$_2$); 0.38 (dd, 10 Hz, 5 Hz, 1H, CH_2═CHPh, trans); 0.94 (d, 7 Hz, 3H, CH*Me*$_2$); not located (CH*Me*$_2$); not located (CH_2═CHPh, cis); not located (C*H*Me_2); not located (CH_2═C*H*Ph); 4.15, 4.46, 4.67, 4.76, 4.92, 5.21, 5.32 (m, 1H, Cp). ^{13}C NMR (benzene-d_6): δ −5.40 (Si*Me*$_2$); −4.71 (Si*Me*$_2$); 18.77 (*C*H_2═CHPh); 23.32 (*C*HMe_2); 24.36 (CH*Me*$_2$); 27.03 (CH*Me*$_2$); 39.21 (CH_2═*C*HPh); 89.41, 90.51, 92.66, 95.20, 100.53, 105.09, 112.02, 137.66 (Cp); 122.34 (C_6H_5, para); not located (C_6H_5, ortho); not located (C_6H_5, meta); 154.24 (C_6H_5, ipso).

[Me_2Si(η^5-C_5H_4)(η^5-C_5H_3-3-$CHMe_2$)]Ta(η^2-CH_2CHPh)H (19a−c). This compound was prepared in a manner similar to that for **11**, employing 0.400 g (0.914 mmol) of **7** and 2.28 mL (2.3 mmol) of 1.0 M $PhCH_2CH_2MgCl$ in THF solution. A golden yellow solid identified as **19** was obtained by slow cooling of a petroleum ether solution followed by filtration (0.120 g, 25.6%). Anal. Calcd for $TaSiC_{23}H_{29}$: C, 53.69; H, 5.68. Found: C, 53.12; H, 5.82%.

Major Isomer 19a. Yield: 54%. ^{1}H NMR (benzene-d_6): δ −1.53 (s, 1H, Ta−*H*); −0.03 (s, 3H, Si*Me*$_2$); 0.09 (s, 3H, Si*Me*$_2$); 1.26 (d, 7 Hz, 3H, CH*Me*$_2$); 1.34 (d, 7 Hz, 3H, CH*Me*$_2$); 2.92 (sept, 6.5 Hz, 1H, C*H*Me_2); 3.56 (m, 1H, CH_2═CHPh, cis); 3.59 (m, 1H, CH_2═CHPh, trans); 3.10 (t, 10 Hz, 1H, CH_2═C*H*Ph);

4.29, 4.33, 5.17, 5.23, 5.28, 5.56, 5.61 (m, 1H, Cp). ^{13}C NMR (benzene-d_6): δ −6.75 (Si*Me*$_2$); −4.36 (Si*Me*$_2$); 13.77 (*C*H$_2$=CHPh); 30.11 (CH$_2$=*C*HPh); 21.70 (C*Me*$_2$); 24.26 (CH*Me*$_2$); 29.09 (*C*HMe$_2$); 83.12, 86.05, 93.46, 95.19, 105.34, 110.55, 4 not located (Cp); 121.90 (C$_6$H$_5$, meta); 136.79 (C$_6$H$_5$, ortho); 154.81 (C$_6$H$_5$, para); not located (C$_6$H$_5$, ipso).

Minor Isomer 19b. Yield: 36%. ^{1}H NMR (benzene-d_6): δ −1.69 (s, 1H, Ta−*H*); −0.01 (s, 3H, Si*Me*$_2$); 0.093 (s, 3H, Si*Me*$_2$); 1.25 (d, 7 Hz, 3H, CH*Me*$_2$); 0.76 (d, 7 Hz, 3H, CH*Me*$_2$); 1.76 (sept, 6.5 Hz, 1H, C*H*Me$_2$); 3.48 (m, 1H, C*H*$_2$=CHPh, cis); 3.48 (m, 1H, C*H*$_2$=CHPh); 3.10 (t, 10 Hz, 1H, CH$_2$=C*H*Ph); 4.24, 4.29, 4.32, 5.21, 5.27, 5.62, 6.04 (m, 1H, Cp). ^{13}C NMR (benzene-d_6): δ −6.92 (Si*Me*$_2$); −4.10 (Si*Me*$_2$); 14.26 (*C*H$_2$=CHPh); 28.65 (CH$_2$=*C*HPh); 24.22 (C*Me*$_2$); 25.48 (CH*Me*$_2$); 26.31 (*C*HMe$_2$); 80.72, 84.27, 94.67, 95.66, 104.79, 106.37, 107.73, 110.34 (Cp); 121.54 (C$_6$H$_5$, meta); 138.88 (C$_6$H$_5$, ortho); 153.84 (C$_6$H$_5$, para); not located (C$_6$H$_5$, ipso).

Trace Isomer 19c. Yield: 10%. ^{1}H NMR (benzene-d_6): δ −1.74 (s, 1H, Ta−*H*); −0.04 (s, 3H, Si*Me*$_2$); 0.06 (s, 3H, Si*Me*$_2$); 0.92 (d, 7 Hz, 3H, CH*Me*$_2$); 1.13 (d, 7 Hz, 3H, CH*Me*$_2$); 2.40 (sept, 6.5 Hz, 1H, C*H*Me$_2$); not located (m, 2H, C*H*$_2$=CHPh); 4.12 (t, 10 Hz, 1H, CH$_2$=C*H*Ph); 4.67, 4.69, 4.99, 5.34, 5.36, 2 not located (m, 1H, Cp). ^{13}C NMR (benzene-d_6): δ −5.20 (Si*Me*$_2$); −6.02 (Si*Me*$_2$); 11.90 (*C*H$_2$=CHPh); 30.61 (CH$_2$=*C*HPh); 20.28 (C*Me*$_2$); 22.50 (CH*Me*$_2$); not located (*C*HMe$_2$); 87.25, 88.31, 91.15, 91.59, 93.95, 100.24, 104.60, 110.07, 2 not located (Cp); 123.99 (C$_6$H$_5$, meta); not located (C$_6$H$_5$, ortho); not located (C$_6$H$_5$, para); not located (C$_6$H$_5$, ipso).

[Me$_2$Si(η^5-C$_5$H$_4$)(η^5-C$_5$H$_2$-2,4-(CHMe$_2$)$_2$)]Ta(η^2-CH$_2$CHPh)H (20a,b). This compound was prepared in a manner similar to that for **11**, employing 0.385 g (0.737 mmol) of **8** and 1.62 mL (1.6 mmol) of 1.0 M PhCH$_2$CH$_2$MgCl in THF, to yield 0.145 g (35.4%) of **20** as a yellow solid. Anal. Calcd for TaSiC$_{26}$H$_{35}$: C, 56.11; H, 6.34. Found: C, 55.71; H, 6.54.

Major Isomer 20a. Yield: 48%. ^{1}H NMR (benzene-d_6): δ −1.760 (s, 1H, Ta−*H*); 0.172 (s, 3H, Si*Me*$_2$); 0.094 (s, 3H, Si*Me*$_2$); 0.940 (d, 6.5 Hz, 3H, CH*Me*$_2$); 1.06 (d, 6.5 Hz, 3H, CH*Me*$_2$); 1.08 (d, 6.5 Hz, 3H, CH*Me*$_2$); 1.54 (d, 6.5 Hz, 3H, CH*Me*$_2$); 2.61 (sept, 6.5 Hz, 1H, C*H*Me$_2$); 2.68 (sept, 6.5 Hz, 1H, C*H*Me$_2$); styrene resonances not located; 4.46, 4.51, 4.75, 4.85, 4.99, 5.23 (m, 1H, Cp); 6.90 (t, 5 Hz, 1H, C$_6$H$_5$, para); 7.47 (d, 7 Hz, 2H, C$_6$H$_5$, ortho); 7.28 (m, 2H, C$_6$H$_5$, meta). ^{13}C NMR (benzene-d_6): δ −3.82 (Si*Me*$_2$); −3.49 (Si*Me*$_2$); 12.48 (*C*H$_2$=CHPh); 30.73 (CH$_2$=*C*HPh); 21.47 (CH*Me*$_2$); 22.79 (CH*Me*$_2$); 24.24 (CH*Me*$_2$); 27.28 (CH*Me*$_2$); 29.28 (*C*HMe$_2$); 29.64 (*C*HMe$_2$); 88.69, 92.12, 96.08, 104.54, 109.03, 111.11, 113.58, 3 not located (Cp); 126.33 (C$_6$H$_5$, para); 136.96 (C$_6$H$_5$, ortho); 155.99 (C$_6$H$_5$, meta); not located (C$_6$H$_5$, ipso).

Minor Isomer 20b. Yield: 39%. ^{1}H NMR (benzene-d_6): δ −1.719 (s, 1H, Ta−*H*); −0.071 (s, 3H, Si*Me*$_2$); 0.257 (s, 3H, Si*Me*$_2$); 1.01 (d, 6.5 Hz, 3H, CH*Me*$_2$); 1.11 (d, 6.5 Hz, 3H, CH*Me*$_2$); 1.34 (d, 6.5 Hz, 3H, CH*Me*$_2$); 1.44 (d, 6.5 Hz, 3H, CH*Me*$_2$); 2.42 (sept, 7 Hz, 1H, C*H*Me$_2$); 2.91 (sept, 1H, C*H*Me$_2$); styrene resonances not located; 4.68, 4.82, 4.92, 5.07, 5.17, 5.89 (m, 1H, Cp); 6.87 (t, 5 Hz, 1H, C$_6$H$_5$, para); 7.40 (d, 7 Hz, 2H, C$_6$H$_5$, ortho); 7.27 (m, 2H, C$_6$H$_5$, meta). ^{13}C NMR (benzene-d_6): δ −1.94 (Si*Me*$_2$); −5.45 (Si*Me*$_2$); 7.70 (*C*H$_2$=CHPh); 34.05 (CH$_2$=*C*HPh); 18.37 (CH*Me*$_2$); 21.97 (CH*Me*$_2$); 25.78 (CH*Me*$_2$); 28.24 (CH*Me*$_2$); not located (*C*HMe$_2$); not located (*C*HMe$_2$); 86.32, 88.06, 92.94, 94.23, 103.48, 108.65, 112.78, 3 not located (Cp); 125.52 (C$_6$H$_5$, para); 140.03 (C$_6$H$_5$, ortho); not located (C$_6$H$_5$, meta); not located (C$_6$H$_5$, ipso).

[Me$_2$Si(η^5-C$_5$H$_4$)(η^5-C$_5$H$_3$-3-CMe$_3$)]Nb(η^2-CH$_2$CHPh)H (21a,b). This compound was prepared in a manner similar to that for **11**, employing 0.205 g (0.506 mmol) of **2** and 1.11 mL (1.1 mmol) of a 1.0 M PhCH$_2$CH$_2$MgCl solution in THF. Extraction with petroleum ether followed by cooling to −40 °C afforded 0.054 g (24%) of a crystalline yellow solid identified as **21**.

Major Isomer 21a. Yield: 90%. ^{1}H NMR (toluene-d_8): δ −2.07 (s, 1H, Nb−*H*); −0.01 (s, 3H, Si*Me*$_2$); 0.12 (s, 3H, Si*Me*$_2$); 0.99 (dd, 10 Hz, 5 Hz, 1H, C*H*$_2$=CHPh, trans); 1.34 (s, 9H, C*Me*$_3$); 1.42 (dd, 13 Hz, 5 Hz, 1H, C*H*$_2$=CHPh, cis); 3.53 (dd, 13 Hz, 10 Hz, 1H, CH$_2$=C*H*Ph); 3.25, 3.44, 4.13, 4.18, 5.16, 5.25, 5.49 (m, 1H, Cp). ^{13}C NMR (toluene-d_8): δ −6.94 (Si*Me*$_2$); −4.13 (Si*Me*$_2$); 20.96 (*C*H$_2$=CHPh); 32.13 (*C*Me$_3$); 32.21 (C*Me*$_3$); 37.81 (CH$_2$=*C*HPh); 73.00, 73.94, 82.70, 86.73, 96.48, 94.62, 104.20, 104.62, 111.90, 143.06 (Cp); 121.97 (C$_6$H$_5$, para); 127.28 (C$_6$H$_5$, ortho); 127.53 (C$_6$H$_5$, meta); 153.23 (C$_6$H$_5$, ipso).

Minor Isomer 21b. Yield: 10%. ^{1}H NMR (toluene-d_8): δ −1.98 (s, 1H, Nb−*H*); 0.05 (s, 3H, Si*Me*$_2$); 0.15 (s, 3H, Si*Me*$_2$); 0.83 (s, 9H, C*Me*$_3$); not located (1H, C*H*$_2$=CHPh, trans); not located (1H, C*H*$_2$=CHPh, cis); 3.18 (dd, 13 Hz, 10 Hz, 1H, CH$_2$=C*H*Ph); 3.07, 3.41, 4.00, 4.07, 5.09, 5.55, 6.13 (m, 1H, Cp). ^{13}C NMR (toluene-d_8): δ −7.09 (Si*Me*$_2$); −3.51 (Si*Me*$_2$); not located (*C*H$_2$=CHPh); not located (*C*Me$_3$); 32.83 (C*Me*$_3$); 35.29 (CH$_2$=*C*HPh); 83.45, 85.24, 96.00, 100.23, 103.88, 106.11, 107.25, 121.59; 2 not located (Cp); not located (C$_6$H$_5$, ortho); not located (C$_6$H$_5$, meta); not located (C$_6$H$_5$, para); not located (C$_6$H$_5$, ipso).

[Me$_2$Si(η^5-C$_5$H$_4$)(η^5-C$_5$H$_3$-3-CMe$_3$)]Ta(η^2-CH$_2$CHPh)H (22). This complex was prepared in a manner analogous to that for **11**, employing 0.500 g (0.935 mmol) of **9** and 2.10 mL (2.1 mmol) of 1.0 M PhCH$_2$CH$_2$MgCl solution in THF. Cooling a concentrated petroleum ether solution affords 0.120 g (22.5%) of a yellow solid identified as **22**. ^{1}H NMR (benzene-d_6): δ −1.602 (s, 1H, Ta−*H*); −0.0375 (s, 3H, Si*Me*$_3$); 0.0785 (s, 3H, Si*Me*$_3$); 1.41 (s, 9H, C*Me*$_3$); 0.928 (m, 1H, C*H*$_2$=CHPh); 1.54 (m,1H, C*H*$_2$=CHPh); 3.142 (t, 12.2 Hz, 1H, CH$_2$=C*H*Ph); 3.33, 3.46, 4.06, 4.17, 5.27, 5.46, 5.60 (m, 1H, Cp). ^{13}C NMR (benzene-d_6): δ −7.10 (Si*Me*$_2$); −4.15 (Si*Me*$_2$); 14.90 (*C*H$_2$=CHPh); 28.68 (CH$_2$=*C*HPh); 31.73 (C*Me*$_3$); 143.59 (*C*Me$_3$); 72.39, 73.32, 80.52, 84.60, 94.59, 96.27, 102.40, 105.11, 2 not located (Cp); 109.73 (C$_6$H$_5$, para); 121.96 (C$_6$H$_5$, ortho), 154.63 (C$_6$H$_5$, meta); not located (C$_6$H$_5$, ipso).

[(1,2-SiMe$_2$)$_2$(η^2-C$_5$H-3,5-(CHMe$_2$)$_2$)(η^5-C$_5$H$_2$-4-CMe$_3$)]Ta(CH$_3$)$_3$ (23). A 250 mL round-bottom flask equipped with stir bar was charged with K$_2$tBuThp (1.05 g, 2.27 mmol), and a medium swivel frit assembly was attached. A 50 mL round-bottom flask equipped with stir bar was charged with TaCl$_2$Me$_3$ (0.674 g, 2.27 mmol), and a 180° needle valve was attached. On the vacuum line, Et$_2$O (250 mL) was added to the swivel frit assembly by vacuum transfer to provide an off-white slurry, and Et$_2$O (25 mL) was added to the TaCl$_2$Me$_3$-containing assembly by vacuum transfer to provide a bright yellow solution. The K$_2$tBuThp slurry was cooled to −78 °C, and the solution of TaCl$_2$Me$_3$ was slowly added via cannula transfer. After 15 min of stirring at −78 °C, the dry ice/acetone bath was replaced with a 0 °C ice/water bath and the reaction apparatus was covered in foil to exclude light. The reaction mixture was stirred for 3 h, and then an orange solution was filtered away from an off-white solid. The solid was washed with Et$_2$O (3 × 25 mL), and solvent was removed in vacuo to provide an orange residue in 25.6% yield (0.354 g). ^{1}H NMR (benzene-d_6): δ 0.38 (s, 6H, (C*H*$_3$)$_2$Si); 0.48 (s, 6H, (C*H*$_3$)$_2$Si); 1.12 (s, 9H, (C*H*$_3$)$_3$C); 1.16 (d, 6H, (C*H*$_3$)$_2$CH, 6.6 Hz); 1.38 (d, 6H, (C*H*$_3$)$_2$CH, 6.9 Hz); 1.49 (s, 9H, Ta−C*H*$_3$); 2.72 (m, 2H, (CH$_3$)$_2$C*H*, 6.6 Hz); 6.51 (s, 1H, Cp); 6.59 (s, 1H, Cp). ^{13}C NMR (benzene-d_6): δ −28.52 (Ta−*C*H$_3$); −0.60, 5.24 ((*C*H$_3$)$_2$Si); 21.61, 25.39, 31.63 ((CH$_3$)$_2$*C*H); 31.93 ((*C*H$_3$)$_3$C); 32.67 ((CH$_3$)$_3$*C*); 73.99, 74.05, 75.83, 75.88 (*C*$_5$H$_1$); 102.36, 118.32, 123.41, 129.63 (*C*$_5$H$_2$).

[(1,2-SiMe$_2$)$_2$(η^5-C$_5$H-3,5-(CHMe$_2$)$_2$)(η^5-C$_5$H$_2$-4-CMe$_3$)]Ta(CH$_2$)CH$_3$ (24). A 250 mL round-bottom flask equipped with stir bar was charged with K$_2$tBuThp (2.68 g, 5.82 mmol) and TaCl$_2$Me$_3$ (1.73 g, 5.82 mmol), and a 180° needle valve was attached. On the vacuum line, 125 mL of toluene was added to the reaction flask by vacuum transfer at −78 °C. The dry ice/acetone cooling bath was removed, and the reaction mixture was warmed slowly to 25 °C. The reaction mixture was stirred for 72 h, and then the solvent was removed in vacuo. In the drybox, Et$_2$O (150 mL) was added to the reaction mixture and

Table 1. X-ray Experimental Data[a]

	12	19b	20a	21a	22	24
formula	$C_{18}H_{27}NbSi$	$C_{23}H_{29}SiTa$	$C_{26}H_{35}SiTa$	$C_{24}H_{31}NbSi$	$C_{24}H_{31}SiTa$	$C_{26}H_{43}Si_2Ta$
fw	364.40	514.50	556.58	440.49	528.53	592.73
cryst syst	monoclinic	monoclinic	triclinic	triclinic	triclinic	monoclinic
space group	$P2_1/c$ (No. 14)	$P2_1/n$ (No. 14)	$P\bar{1}$ (No. 2)	$P\bar{1}$ (No. 2)	$P\bar{1}$ (No. 2)	$P2_1/m$ (No. 11)
a, Å	9.2022(6)	14.5277(9)	9.2305(8)	10.3001(11)	10.2246(18)	8.508(3)
b, Å	21.1677(14)	6.6809(4)	10.1700(9)	10.5568(11)	10.5009(18)	16.123(6)
c, Å	9.2632(6)	21.0147(12)	12.9218(12)	11.2207(12)	11.1345(19)	9.984(3)
α, deg	90	90	90.336(1)	74.243(2)	74.140(3)	90
β, deg	108.940(1)	99.331(1)	104.187(1)	84.333(2)	84.118(3)	112.39(3)
γ, deg	90	90	100.414(1)	66.971(2)	66.993(2)	90
V, Å^3	1706.68(19)	2012.7(2)	1155.05(18)	1080.6(2)	1058.5(3)	1266.3(8)
Z	4	4	2	2	2	2
ρ_{calcd}, g/cm^3	1.418	1.698	1.600	1.354	1.658	1.555
μ, mm^{-1}	0.76	5.52	4.82	0.62	5.25	4.45
F_{000}	760	1016	556	460	524	600
cryst shape	lozenge	needle	thick blade	lozenge	stacked plates	twinned plate
cryst color	yellow	yellow	yellow	yellow	yellow	golden orange
cryst size, mm	0.10 × 0.26 × 0.26	0.04 × 0.08 × 0.12	0.14 × 0.18 × 0.33	0.14 × 0.20 × 0.31	0.03 × 0.15 × 0.26	0.07 × 0.18 × 0.19
T, K	98	98	95	98	93	84
type of diffractometer			SMART 1000 ccd			CAD-4
θ range, deg	1.9−28.5	1.6−27.5	2.0−28.2	1.9−28.5	1.9−28.2	2.2−25
h,k,l limits	−12 to +12; −28 to +28; −12 to +12	−18 to +18; −8 to +8; −27 to +27	−11 to +12; −13 to +13; −17 to +16	−13 to +13; −13 to +14; −14 to +14	−13 to +13; −13 to +13; −14 to +14	−10 to +10; −19 to +19; −11 to +11
no. of data measd	25 466	34 421	10 310	22 478	19 961	11 978
no. of unique data	4105	4617	5071	5072	4860	1651
no. of data, $F_o > 4\sigma(F_o)$	3597	3186	4848	4407	4347	1576
no. of params/restraints	289/0	226/0	389/0	359/0	257/0	140/0
R1,[b] wR2[c] (all data	0.028, 0.048	0.084, 0.072	0.027, 0.050	0.037, 0.051	0.052, 0.114	0.030, 0.066
R1,[b] wR2[c] ($F_o > 4\sigma(F_o)$)	0.023, 0.048	0.042, 0.066	0.026, 0.050	0.031, 0.050	0.047, 0.112	0.027, 0.066
GOF[d] on F^2	1.84	1.58	2.19	1.53	1.29	2.38
$\Delta\rho_{max}$, $\Delta\rho_{min}$, e Å^{-3}	0.51, −0.37	1.92, −1.84	2.33, −1.76	0.60, −0.43	3.62, −3.29	1.58, −0.82

[a] All data were collected with graphite-monochromated Mo Kα radiation ($\lambda = 0.710\ 73$ Å). The structure of **23** is included in the Supporting Information. [b] $R1 = \sum||F_o| - |F_c||/\sum|F_o|$. [c] $wR2 = \{\sum[w(F_o^2 - F_c^2)^2]/\sum[w(F_o^2)^2]\}^{1/2}$. [d] $GOF = S = \{\sum[w(F_o^2 - F_c^2)^2]/(n - p)\}^{1/2}$.

then the contents were filtered through a bed of Celite and washed with Et_2O (5 × 25 mL). A 250 mL round-bottom flask equipped with stir bar was charged with the brown mother liquor, and a fine swivel frit assembly was attached. On the vacuum line the Et_2O was removed in vacuo and then 50 mL of pentane was added by vacuum transfer. A brown supernatant was filtered away from a yellow precipitate, and the solid was washed with pentane (2 × 25 mL). Solvent was removed in vacuo to provide **24** as a mustard yellow solid in 20.9% yield (0.723 g). ^{1}H NMR (benzene-d_6): δ 0.24 (s, 3H, Si*Me*$_2$); 0.36 (s, 3H, Si*Me*$_2$); 0.44 (s, 3H, Si*Me*$_2$); 0.45 (s, 3H, Ta−C*H*$_3$); 0.51 (s, 3H, Si*Me*$_2$); 1.10 (d, 7.0 Hz, 3H, CH*Me*$_2$); 1.12 (d, 5.9 Hz, 3H, CH*Me*$_2$); 1.16 (d, 6.6 Hz, 3H, CH*Me*$_2$); 1.39 (d, 6.6 Hz, 3H, CH*Me*$_2$); 1.49 (s, 9H, C*Me*$_3$); 2.55 (m, 5.4 Hz, 1H, C*H*Me$_2$); 3.38 (m, 5.7 Hz, 1H, C*H*Me$_2$); 5.91 (s, 2H, Cp); 6.57 (s, 1H, Cp); 9.30 (d, 9.8 Hz, 1H, Ta=C*H*$_2$); 9.58 (d, 9.8 Hz, 1H, Ta=C*H*$_2$). ^{13}C NMR (benzene-d_6): δ −2.01 (Ta−*C*H$_3$); −1.82, −1.40, 3.78, 4.00 (Si*Me*$_2$); 21.61, 22.20, 28.04, 28.90, 30.18, 30.64 (*C*H*Me*$_2$); 31.16 (C*Me*$_3$), 33.05 (*C*Me$_3$); 102.71, 118.67, 123.74 (Cp); 211.26 (Ta=*C*H$_2$).

[(1,2-SiMe$_2$)$_2$(η^5-C$_5$H-3,5-(CHMe$_2$)$_2$)(η^5-C$_5$H$_2$-4-CMe$_3$)]Ta-(η^2-CH$_2$CH$_2$)H (25). A 25 mL round-bottom flask equipped with stir bar was charged with **24** (0.121 g, 0.203 mmol), and a reflux condenser and 180° needle valve were attached. On the vacuum line, 15 mL of toluene was added to the reaction flask by vacuum transfer, providing a yellow-brown solution. The apparatus was back-filled with Ar and then heated to reflux. After 72 h at reflux, the toluene was removed in vacuo and pentane (10 mL) was added by vacuum transfer and then removed in vacuo to provide a brown solid in 96.5% yield (0.116 g). ^{1}H NMR (benzene-d_6): δ −2.06 (s, 1 H, Ta−*H*); 0.43 (s, 3H, Si*Me*$_2$); 0.55 (s, 3H, Si*Me*$_2$); 0.63 (s, 3H, Si*Me*$_2$); 0.68 (s, 3H, Si*Me*$_2$); 0.78 (d, 6.6 Hz, 3H, CH*Me*$_2$); 0.97 (s, 9H, C*Me*$_3$), 1.10 (d, 7.3 Hz, 3H, CH*Me*$_2$); 1.11 (d, 7.2 Hz, 3H, CH*Me*$_2$); 1.37 (d, 6.6 Hz, 3H, CH*Me*$_2$); 2.97 (m, 6.9 Hz, 1H, C*H*Me$_2$); 3.40 (m, 6.5 Hz, 1H, C*H*Me$_2$); 4.13, 5.81, 6.35 (s, 1H, Cp); C*H*$_2$=C*H*$_2$ not located. ^{13}C NMR (benzene-d_6): δ −1.53, −0.78, 5.00, 6.14 Si*Me*$_2$); 21.75, 23.08 (*C*H$_2$=*C*H$_2$); 28.67, 29.18, 29.63, 30.44, 31.93, 33.04, 30.83 (CH*Me*$_2$, *CMe*$_3$); 98.36, 110.66, 111.18, 137.72 (Cp).

[(1,2-SiMe$_2$)$_2$(η^5-C$_5$H-3,5-(CHMe$_2$)$_2$)(η^5-C$_5$H$_2$-4-CMe$_3$)]Ta-(η^2-CH$_2$CHCH$_3$)H (26). A J. Young NMR tube was charged with **25** (10.8 mg, 0.0182 mmol), and this compound was dissolved in benzene-d_6 to provide a red-brown solution. On the vacuum line, the solution was frozen at −196 °C and the NMR tube was degassed. Propylene (0.182 mmol) was condensed into the NMR tube at this temperature, and the tube was closed and warmed to 25 °C. After 19 days at 25 °C, a 10:1 ratio of **26** to **25** is observed. ^{1}H NMR (benzene-d_6): δ −1.86 (s, 1 H, Ta−*H*); −0.27 (br s, 1H, CH$_2$=C*H*(CH$_3$)); −0.19 (m, 2H, C*H*$_2$=CH(CH$_3$)); 0.42 (s, 3H, Si*Me*$_2$); 0.54 (s, 3H, Si*Me*$_2$); 0.61 (s, 3H, Si*Me*$_2$); 0.66 (s, 3H, Si*Me*$_2$); 0.97 (d, 6.8 Hz, 3H, CH*Me*$_2$); 1.01 (s, 9H, C*Me*$_3$); 1.11 (d, 6.9 Hz, 3H, CH*Me*$_2$); 1.16 (d, 7.1 Hz, 3H, CH*Me*$_2$); 1.35 (d, 6.6 Hz, 3H, CH*Me*$_2$); 2.32 (d, 6.6 Hz, 3H, CH$_2$=CH(C*H*$_3$)); 3.10 (m, 6.3 Hz, 1H, C*H*Me$_2$); 3.38 (m, 7.0 Hz, 1H, C*H*Me$_2$); 4.19, 5.55, 6.32 (s, 1H, Cp). ^{13}C NMR (benzene-d_6): δ −1.56, −0.91, 3.94, 4.17 (Si*Me*$_2$); 13.95, 21.77, 21.91 (*C*H$_2$=*C*H(CH$_3$)); 23.10, 28.68, 29.19, 29.40, 29.51, 30.67, 30.83, 32.03 (*C*H*Me*$_2$, *CMe*$_3$); 98.32, 110.14, 112.65, 126.66, 139.34, 147.42 (Cp).

[(1,2-SiMe$_2$)$_2$(η^5-C$_5$H-3,5-(CHMe$_2$)$_2$)(η^5-C$_5$H$_2$-4-CMe$_3$)]Ta-(η^2-CH$_2$CHPh)H (27). A J. Young NMR tube was charged with **25** (20.0 mg, 0.0337 mmol), and this compound was dissolved in benzene-d_6 to provide a red-brown solution. A small amount of a styrene/benzene-d_6 solution was added (0.4044 mmol, 12 equiv), and the reaction was monitored at 25 °C by ^{1}H NMR spectroscopy. After 79 days at 25 °C, a 10:1 ratio of **27** to **25** is observed. ^{1}H NMR (benzene-d_6): δ −1.10 (s, 1 H, Ta−*H*); 0.35 (s, 3H, Si*Me*$_2$); 0.48 (s, 3H, Si*Me*$_2$); 0.56 (s, 3H, Si*Me*$_2$); 0.58 (s, 3H, Si*Me*$_2$); 0.60 (d, 6.7 Hz, 3H, CH*Me*$_2$);

0.95 (d, 7.0 Hz, 3H, CH*Me*$_2$); 1.08 (s, 9H, C*Me*$_3$); 1.14 (d, 7.1 Hz, 3H, CH*Me*$_2$); 1.18 (d, 6.7 Hz, 3H, CH*Me*$_2$); 1.29 (m, 2H overlapping, C*H*$_2$═CHPh); 2.80 (t, 12.5 Hz, 1H, CH$_2$═C*H*Ph); 3.19 (m, 7.2 Hz, 2H overlapping, C*H*Me$_2$); 3.63, 5.62, 6.43 (s, 1H, Cp); 6.82 (t, 7.1 Hz, 1H, C$_6$H$_5$, para); 7.23 (t, 8.0 Hz, 2H, C$_6$H$_5$, meta); 7.47 (d, 7.9 Hz, 2H, C$_6$H$_5$, ortho). ^{13}C NMR (benzene-d_6): δ −1.84, −0.71, 3.89, 8.82 (Si*Me*$_2$); 21.29, 22.40 (*C*H$_2$═*C*HPh); 28.91, 29.42, 29.80, 31.26, 32.26, 33.13 (*CHMe*$_2$); 30.67 (C*Me*$_3$); 78.67, 81.34, 87.07, 102.93, 110.45, 112.08, 121.52, 126.31, 2 not located (Cp); not located (*C*Me$_3$); 142.41, 148.40, 156.48, 1 not located (C$_6$H$_5$).

Crystallography. Crystal data and intensity collection and refinement details are presented in Table 1 for compounds **12**, **19b**, **20a**, **21a**, **22**, and **24**.

Data Collection and Processing. Data for compound **24** were collected on a Nonius CAD 4 serial diffractometer; data for all other compounds were collected on a Bruker SMART 1000 area detector running SMART.[31] Both diffractometers were equipped with Crystal Logic CL24 low-temperature devices, and all data sets were collected at low temperature. Both diffractometers used graphite-monochromated Mo Kα radiation with λ = 0.710 73 Å.

CCD samples (**12**, **19b**, **20a**, **21a**, **22**): The crystals were mounted on glass fibers with Paratone-N oil. Data were collected as ω-scans at three to six values (depending on the sample) of φ. For all crystals, the detector was 5 cm (nominal) distant at a θ angle of −28°. The data were processed with SAINT.[31]

CAD4 sample (**24**): The crystals were mounted on glass fibers with Paratone-N oil. Indexing problems with several crystals suggested twinning. Finally a crystal was found for which a unit cell could be determined. Although this crystal was also twinned, orientation matrices were obtained for both twin components. The twin can be described as a reflection twin across the (100) plane. The unit cell was calculated from 25 centered reflections. Approximately four sets of data were collected with 1.0 ω-scans. CRYM[32] programs were used to apply Lorentz and polarization factors to the data set and to merge the multiples in point group 2/*m*. Data which agreed poorly in a preliminary merging were recollected. The individual backgrounds were replaced by a background function of 2θ derived from those reflections with $I < 3\sigma(I)$. Weights w were calculated as $1/\sigma^2(F_o^2)$; variances ($\sigma^2(F_o^2)$) were derived from counting statistics plus an additional term, $(0.014I)^2$; variances of the merged data were obtained by propagation of error plus another additional term, $(0.014\langle I\rangle)^2$.

Structure Analysis and Refinement. SHELXTL v5.1[31] was used to solve, via direct methods or by the Patterson method, and to refine all structures using full-matrix least squares. All non-hydrogen atoms were refined anisotropically. For **12**, there is one molecule in the asymmetric unit. All hydrogen atoms, including the hydride, were refined isotropically. For **19b**, there is one molecule in the asymmetric unit. SADABS was used to correct for absorption. Hydrogen atoms were placed at calculated positions with U_{iso} values of 120% of U_{eq} of the attached atom. The hydride could not be located in a difference map and was not included in the refinement. There were unindexed peaks in the data frames, and this was probably not a single crystal; consistent with this interpretation, some of the largest peaks in the final difference map were not next to the Ta atom. For **20a**, there is one molecule in the asymmetric unit. A satisfactory absorption correction was obtained using SADABS. The coordinates and the temperature factor of the hydride on the metal center were fixed during the final least squares. All other hydrogen atoms were freely refined. For **21a**, there is one molecule in the asymmetric unit. All hydrogen atoms, including the hydride, were refined isotropically. Compound **22** (Ta) is isostructural with **21a** (Nb); therefore, there is one molecule in the asymmetric unit. The hydrogen atoms were placed at calculated positions and constrained to a reasonable geometry; the hydride parameters were not refined. For **24**, there is a half-molecule in the asymmetric unit. The molecule lies on a mirror plane containing the Ta atom and bisecting the two Cp rings. This crystallographically imposed symmetry has the unfortunate consequence of confusing the chemically inequivalent ═CH$_2$ and −CH$_3$ ligands. All hydrogen atoms were placed at calculated positions with U_{iso} values fixed at 120% of the U_{eq} value of the attached atom. The *tert*-butyl group is also disordered about the mirror plane, as is seen in similar compounds. The first attempts at refinement included all measured reflections; those reflections which presumably included overlap between the two twin components were given two sets of indices corresponding to the two twins. Various criteria were used to identify overlapping reflections. However, none of these approaches were particularly successful, presumably since most reflections do not perfectly coincide. Finally, all reflections with l = 3, 6, 9, and 11 were removed from the data set; these reflections transform with h' deviating from integral values by ∼0.05, 0.10, 0.15, and 0.15, respectively. Therefore, only the $hk0$ reflections, which overlap perfectly with the $h-k0$ reflections of the twin, contain any twin contribution. The $h-k0$ reflections were added as the symmetry-equivalent $hk0$ form. A twin parameter relating the relative contributions of the two components was included in the least-squares matrix; the fractional amount of the minor component was refined to 0.168(4).

Acknowledgment. This work has been supported by the USDOE Office of Basic Energy Sciences (Grant No. DE-FG03-85ER13431) and Exxon Chemicals America. L.J.A. wishes to thank the National Science Foundation for a Graduate Research Fellowship.

Supporting Information Available: Text giving details of the structure determination and tables of atomic coordinates, all bond distances and angles, and anisotropic displacement parameters for all structurally characterized complexes, and a labeled drawing for complex **23**. This material is available free of charge via the Internet at http://pubs.acs.org.[33]

OM020628D

(31) SMART, SAINT, and SHELXTL; Bruker AXS Inc., Madison, WI, 1999.

(32) Duchamp, D. J. American Crystallographic Association Meeting, Bozeman, MT, 1964; Paper B14, p 29.

(33) Crystallographic data for the structures of **12** (CCDC 147070), **19b** (CCDC 162232), **20a** (CCDC 140682), **21a** (CCDC 147250), **22** (CCDC 142045), **23** (CCDC 147415), and **24** (CCDC 147413) have been deposited with the Cambridge Crystallographic Data Centre as supplementary publications. These data can be obtained free of charge via http://www.ccdc.cam.ac.uk/conts/retrieving.html (or from the Cambridge Crystallographic Data Centre, 12 Union Road, Cambridge CB2 1EZ, U.K.; fax +44 1223 336033; email deposit@ccdc.cam.ac.uk). Structure factors are available electronically by e-mail: xray@caltech.edu.